A Description of Seismicity Based on Non-extensive Statistical Physics: A Review

Filippos Vallianatos, Georgios Michas and Giorgos Papadakis

1 Introduction

Earthquakes have always been one the most intriguing natural phenomena for mankind. The abruptness of the shaking ground and the devastating consequences for the human environment were always attracting people's fear and wonder. Despite the large amount of effort that has been dedicated in understanding the physical processes that lead to the birth of an earthquake and the significant progress that has been achieved in this field, the prediction of an upcoming earthquake still remains a challenging question (Nature debates 1999).

Concerning the physics of earthquakes, many questions have not yet been answered since the phenomenon is subjected to many uncertainties and degrees of freedom. It is true that we have a good understanding of the propagation of seismic waves through the Earth and that given a large set of seismographic records, we are able to reconstruct a posteriori the history of the fault rupture. However, when we consider the physical processes leading to the initiation of a rupture with a subsequent slip and its growth through a fault system, giving rise to an earthquake, then our knowledge is really limited. Not only the friction law and the rules that govern rupture evolution are largely unknown, but also the role of many other processes such as plasticity, fluid migration, chemical reactions, etc., and the couplings among them, remain unclear (Main et al. 1989, 1992; Sammonds 2005; Sammonds and Ohnaka 1998; Vallianatos et al. 2004).

F. Vallianatos (✉)
Technological Educational Institute of Crete, Laboratory of Geophysics and Seismology, Chania, 73100 Crete, Greece
e-mail: fvallian@chania.teicrete.gr

F. Vallianatos · G. Michas · G. Papadakis
Institute for Risk and Disaster Reduction, University College London, Gower Street, London, WC1E 6BT, UK

S. D'Amico (ed.), *Earthquakes and Their Impact on Society*,
Springer Natural Hazards, DOI 10.1007/978-3-319-21753-6_1

Despite the extreme complexity that characterizes the mechanism of the earthquake generation process, simple phenomenology seems to apply in the collective properties of seismicity. Fault and earthquake populations present scaling relations that seem to be universal in the sense that are appearing in a variety of tectonic environments and scales that vary from the laboratory, to major fault zones and plate boundaries. The best known is the Gutenberg-Richter scaling relation (Gutenberg and Richter 1944) that indicates power-law scaling for the earthquake size distribution. Short and long-term clustering, power-law scaling and scale-invariance have also been exhibited in the temporal evolution of seismicity (Kagan and Jackson 1991). In addition, earthquakes exhibit fractal spatial distribution of epicenters and they occur on fractal-like structure of faults (Turcotte 1997). All these properties provide observational evidence for earthquakes as a nonlinear dynamic process (Kagan 1994).

Due to these properties, concepts such as fractals, multi-fractals, non-linear processes and chaotic dynamical systems are becoming increasingly fundamental for analyzing data and understanding processes in geosciences. In recent years, there is a growing interest on approaching seismicity and other natural hazards, regarding the science of complex systems and the fractal nature of these phenomena (Bak and Tang 1989; Bak et al. 1988; Vallianatos 2009). In the context of critical point phenomena (see Sornette 2004), "self-organized criticality" (SOC) has been proposed by Bak et al. (1987) as a possible driving mechanism that produce the scale-invariant properties of the earthquake populations, such as the G-R scaling relation (see also Bak and Tang 1989; Sornette and Sornette 1989). According to this theory, Earth's crust is in a near critical state that spontaneously organizes into an out-of-equilibrium state to produce earthquakes of fractal size distributions.

Regarding the physics of "many" earthquakes and how this can be derived from first principles, one may wonder:

- How can the collective properties of a set formed by all earthquakes in a given region, be derived?
- How does the structure of seismicity, as formed by all earthquakes, depends on its elementary constituents—the earthquakes? What are these properties?

It may be that these collective properties are largely independent on the physics of the individual earthquakes, in the same way that many of the properties of a gas or a solid do not depend on the constitution of its elementary units. It is natural then to consider that the physics of many earthquakes has to be studied with a different approach than the physics of one earthquake and in this sense we can consider *the use of statistical physics not only appropriate but also necessary to understand the collective properties of earthquakes*. A significant attempt is given in a series of works (Main 1996; Main and Al-Kindy 2002; Rundle et al. 1997, 2003) where classic statistical physics are used to describe seismicity. Then a natural question arises. *What type of statistical physics is appropriate to commonly describe effects from the microscale and crack opening level to the level of large earthquakes and plate tectonics?*

An answer to the previous question could be non-extensive statistical physics (NESP), originally introduced by Tsallis (1988). The latter is strongly supported by the fact that this type of statistical mechanics is the appropriate methodological tool to describe entities with (multi) fractal distributions of their elements and where long-range interactions or intermittency are important, as in fracturing phenomena and earthquakes. NESP is based on a generalization of the classic Boltzmann-Gibbs entropy and has the main advantage that it considers all-length scale correlations among the elements of a system, leading to an asymptotic power-law behavior. So far, NESP has found many applications in nonlinear dynamical systems including earthquakes (Tsallis 2009). In a series of recent publications, it has been shown that the collective properties of the earthquake and fault populations from the laboratory scale (Vallianatos et al. 2011a, 2012a, b, 2013; Vallianatos and Triantis, 2012), to local (Michas et al. 2013), regional (Abe and Suzuki 2003, 2005; Telesca 2010a; Papadakis et al. 2013) and global scale (Vallianatos and Sammonds 2013) can be reproduced rather well using the concept of NESP.

In the present chapter, we review some fundamental properties of earthquake physics (in the geodynamic-laboratory scale) and how these are derived by means of non-extensive statistical physics. The aim is to understand aspects of the underlying physics that lead to the evolution of the earthquake phenomenon. We are focused in a variety of scales, from plate tectonics downscaling to rock fractures and laboratory seismology, to understand better the fundamentals of earthquake occurrence and contribute to the seismic hazard assessment, introducing the new topic of non-extensive statistical seismology.

2 Fundamentals of Non-extensive Statistical Physics

Boltzmann-Gibbs (BG) statistical physics is one of the cornerstones of contemporary physics. It establishes a remarkably useful bridge between the mechanical microscopic laws and macroscopic description using classical thermodynamics. The theory centrally addresses the very special stationary state—denominated thermal equilibrium. This macroscopic state has fundamental importance, since it is the foundation in Boltzmann's famous molecular chaos hypothesis made in 1871. However, BG theory is not universal. It has a limited domain of applicability (Tsallis 2009). Outside this domain, its predictions can be slightly or even strongly inadequate. There was a conflict, among many physicists as well as other scientists, that BG mechanics and standard thermodynamics are always valid and universal. It is certainly fair to say that always valid, in precisely the same sense that Newtonian mechanics is always valid; they indeed are. But again in complete analogy with Newtonian mechanics, we can by no means consider them as universal.

Central in BG statistical physics is the associated entropy that for the discrete states of a system has the form

$$S_{BG} = -k_B \sum_{i=1}^{W} p_i \ln p_i, \quad \text{with} \sum_{i=1}^{W} p_i = 1 \tag{2.1}$$

where S_{BG} is Boltzmann-Gibbs entropy, k_B is Boltzmann's constant, p_i is a set of probabilities and W is the total number of microscopic configurations. One of the main characteristics of S_{BG} is additivity, namely the proportionality to the number of the systems' elements. According to this property, for any two probabilistically independent systems A and B, i.e. if the joint probability satisfies $p_{ij}^{A+B} = p_i^A p_j^B (\forall (i,j))$, S_{BG} satisfies

$$S_{BG}(A+B) = S_{BG}(A) + S_{BG}(B). \tag{2.2}$$

Although BG entropy seems the correct one to be used in a large and important class of physical systems with strongly chaotic dynamics (positive maximal Lyapunov exponent), an important class of weakly chaotic systems (where the maximal Lyapunov exponent vanishes) violates this hypothesis. Additionally, if the effective microscopic interactions and memory are short-ranged (for instance Markovian processes) and the boundary conditions are smooth, then BG statistical mechanics seems to correctly describe nature. On the other hand, if some or all of these restrictions are violated (long-range interactions, non-markovian microscopic memory, multifractal boundary conditions and multifractal structures), then another type of statistical mechanics seems appropriate to describe nature (see for instance Zaslavsky 1999; Tsallis 2001).

Naturally, a question arises: Is it possible to address some of these important, though anomalous in the BG sense, situations with concepts and methods similar to those of BG statistical mechanics? Many theoretical, experimental and observational indications are nowadays available and point towards an affirmative answer. To overcome at least some of these anomalies that seem to violate BG statistical mechanics, non-extensive statistical physics (NESP) was proposed by Tsallis in (1988) that recovers the extensive BG as a particular case. The associated generalized entropic form for the discrete case is

$$S_q = k_B \frac{1 - \sum_{i=1}^{W} p_i^q}{q-1}, \quad q \in R \text{ with} \sum_{i=1}^{W} p_i = 1 \tag{2.3}$$

where S_q is Tsallis entropy and q is the entropic index that represents a measure of the non-extensivity of a system. S_q recovers S_{BG} in the limit $q \to 1$. Although Tsallis entropy and Boltzmann-Gibbs entropy share a variety of thermodynamical properties like concavity (relevant for the thermodynamical stability of the system), experimental results, extensivity (relevant for having a natural matching with the entropy as introduced in classical thermodynamics), and finiteness of the entropy production per unit time (relevant for a variety of real situations where the system is

striving to explore its microscopic phase space in order to ultimately approach some kind of stationary state) (see Tsallis 2009 for the full list of these properties), S_{BG} is additive, whereas S_q ($q \neq 1$) is non-additive. This property is directly related to the definition of S_q in Eq. (2.3). Indeed, for any two probabilistically independent systems A and B, i.e. if the joint probability satisfies $p_{ij}^{A+B} = p_i^A p_j^B (\forall (i, j))$, Tsallis entropy S_q satisfies:

$$\frac{S_q(A+B)}{k} = \frac{S_q(A)}{k} + \frac{S_q(B)}{k} + (1-q)\frac{S_q(A)}{k}\frac{S_q(B)}{k}. \tag{2.4}$$

The origin of non-additivity comes from the last term on the right hand side of this equation and is the fundamental principle of non-extensive statistical physics (Tsallis 2009). The cases $q > 1$, $q = 1$ and $q < 1$ correspond to sub-additivity, additivity and super-additivity respectively.

Tsallis idea of introducing the non-additive entropy S_q was inspired by simple physical principles and the multifractal concept (see Tsallis 2009 for a thorough description). A bias in the probabilities of the different states in a system is introduced by using the entropic index q. Given the fact that generically $0 < p_i < 1$, we have that $p_i^q > p_i$ if $q < 1$ and $p_i^q < p_i$ if $q > 1$. Therefore, $q < 1$ enhances the rare events with probabilities close to zero, whereas $q > 1$ enhances the frequent events, i.e., those whose probabilities are close to unity. Following Tsallis (2009), it is natural to introduce an entropic form passed on p_i^q. The entropic form must be invariant under permutation and the simplest expression which is consistent with this has the form $S_q = F\left(\sum_{i=1}^{w} p_i^q\right)$, where $F(x)$ is a continuous function. The simplest form of $F(x)$ is the linear one, leading to $S_q = \mathrm{C}_1 + \mathrm{C}_2 \sum_{i=1}^{w} p_i^q$. As any entropy, S_q must be a measure of disorder leading to $\mathrm{C}_1 + \mathrm{C}_2 = 0$ (Tsallis 2009) and hence $S_q = \mathrm{C}_1\left(1 - \sum_{i=1}^{w} p_i^q\right)$. In the limit $q \rightarrow 1$ the entropic form S_q approaches the Boltzmann-Gibbs expression and the simplest way for this is when $\mathrm{C}_1 = k_B/(q-1)$.

Tsallis entropy is determined by the microscopic dynamics of the system. This point is quite important in practice. If the microscopic dynamics of the system are known, we can determine the corresponding value of entropic index q from the first principles. As it happens, this precise dynamics is most frequently unknown for many natural systems. In this case, a way out that is currently used, is to check the functional forms and then determine the appropriate values of q by fitting. Moreover, there are many complex systems for which one may reasonably argue that they belong to the class that is addressed by non-extensive statistical concepts, but whose microscopic dynamics is inaccessible. For such systems, it appears as a sensible attitude to adopt the mathematical forms that emerge in the theory, e.g. q-exponentials (see below) and then obtain the correct graphs through fitting the corresponding value of q and of similar characteristics.

2.1 Optimizing Tsallis Entropy S_q

Suppose that we have a continuous variable X with a probability distribution $p(X)$. In geophysics, this variable can be for instance seismic moment (M_o), inter-event times (τ) or distances (r) between the successive earthquakes or the length of faults (L) in a given region.

For the probability distribution $p(X)$ of the continuous variable X, Tsallis entropy S_q is given by the integrated formulation as follows:

$$S_q = k_B \frac{1 - \int p^q(X) dX}{q - 1}. \tag{2.1.1}$$

where q the entropic index. In the following we set k_B as unity for the sake of simplicity. We require optimizing S_q under the appropriate constraints. The first constraint refers to the normalization condition of $p(X)$:

$$\int_0^\infty p(X) dX = 1 \tag{2.1.2}$$

The second constraint is the condition about the generalized expectation value (q-expectation value), X_q defined as:

$$X_q = \langle X_q \rangle = \int_0^\infty X P_q(X) dX \tag{2.1.3}$$

where $P_q(X)$ is the escort probability given (Tsallis 2009) as follows:

$$P_q(X) = \frac{p^q(X)}{\int_0^\infty p^q(X) dX} \tag{2.1.4}$$

Using the standard technique of Lagrange multipliers, the following functional is maximized:

$$\Phi(p, a^*, \beta^*) = S_q - a^* \int_0^{x_{\max}} p(X) dX - \beta^* X_q \tag{2.1.5}$$

where α^* and β^* represent the Lagrange multipliers.

Imposing that, $\partial \Phi / \partial p = 0$ we obtain the physical probability:

$$p(X) = \frac{\left[1-(1-q)\beta_q X\right]^{1/1-\mathrm{q}}}{Zq} = \frac{\exp_q(-\beta_q X)}{Z_q} \tag{2.1.6}$$

where the q-exponential function is defined as (see Tsallis 2009 and references therein):

$$\exp_q(X) = \begin{cases} [1+(1-\mathrm{q})\mathrm{X}]^{1/(1-\mathrm{q})} & (1+(1-\mathrm{q})\mathrm{X} \geq 0) \\ 0 & (1+(1-\mathrm{q})\mathrm{X} < 0) \end{cases} \tag{2.1.7}$$

whose inverse is the q-logarithmic function: $ln_q(X) = \frac{1}{1-q}(X^{1-q}-1)$

The denominator of Eq. (2.1.6) is called q-partition function and is defined as:

$$Z_q = \int_0^{x_{\max}} \exp_q(-\beta_q X)dX \tag{2.1.8}$$

where, $\beta_q = \frac{\beta}{c_q+(1-q)\beta X q}$ and $\mathrm{c_q} = \int_0^{x_{max}} p^q(X)dX$

The q-exponential distribution consists a generalization of the Zipf-Mandelbrot distribution (Mandelbrot 1983), where the standard Zipf-Mandelbrot distribution corresponds to the case $q > 1$ (Abe and Suzuki 2003). In the limit $q \rightarrow 1$ the q-exponential and q-logarithmic functions lead to the ordinary exponential and logarithmic functions respectively. If $q > 1$ Eq. (2.1.6) exhibits an asymptotic power-law behavior with slope $-1/(q-1)$. In contrast, for $0 < q < 1$ a cut-off appears (Abe and Suzuki 2003, 2005).

In non-extensive statistical physics it has been proposed that the quantity to be compared with the observed distribution is not the physical probability $p(X)$ but its associated escort distribution (see Abe and Suzuki 2005; Tsallis 2009; Vallianatos 2009). Following the latter approach, the cumulative distribution function is given by the expression

$$P_{cum}(>X) = \int_{X_{min}}^{\infty} P_q^{esc}(X)dX. \tag{2.1.9}$$

Combining the latter definition with the probability function $p(X)$ we obtain

$$\mathrm{P_{cum}}(>\mathrm{X}) = \exp_{\mathrm{q}}(-\mathrm{X}/\mathrm{X_o}), \tag{2.1.10}$$

which after simple algebra leads to $\frac{[P_{cum}(>X)]^{1-q}-1}{1-q} = -\frac{X}{X_o}$. The latter equation implies that after estimating the appropriate q, which describes the distribution of the variable X, the $\ln_q(P_{cum}(>X)) = \frac{[P_{cum}(>X)]^{1-q}-1}{1-q} = \left(-\frac{1}{X_o}\right)X$, which express the

q-logarithmic function, is linear with X with slope $-1/X_o$. In Fig. 1 the q-exponential distribution of Eq. (2.1.10) is plotted for various values of the q index.

In cases where $X > X_{\min}$, the cumulative distribution of X assumes value 1 for $X = X_{\min}$. This implies that the aforementioned equation should be slightly changed (Vallianatos 2013) into the following form, which is more consistent with real observations:

$$P(>X) = \frac{\exp_q(-X/X_o)}{\exp_q(-X_{\min}/X_o)}. \tag{2.1.11}$$

We note that in cases where $X_{\min} \ll X_o$, the latter introduction does not significantly change the estimated results.

An interesting question that is brought forth in NESP is which distribution we shall compare with the observed distribution. The common approach that is most frequently used is the introduction of the escort probability in the second constraint and the optimization of S_q as described earlier. Other forms have been developed and are described thoroughly in Tsallis (2009). Detailed discussions on this subject can be also found in Wada and Scarfone (2005), Ferri et al. (2005), where it was shown that the different forms related to the second constraint of the expectation value are all equivalent and can be transformed one into the other through simple operations defining q s and X_o s. For instance, if we integrate the physical probability given in Eq. (2.1.6) instead of the escort probability (Eq. 2.1.4), we obtain the cumulative probability:

$$P(>X) = \left[1 - (1-q')\frac{X}{X'_o}\right]^{1/(1-q')}, \tag{2.1.12}$$

where $q' = 1/(2-q)$ and $X'_o = (2-q)/X_o$, in relation to q and X_o values in Eq. (2.1.10) (Picoli et al. 2009). If we apply these transformations for q' and X'_o, the following form of the cumulative distribution $P(>X)$ is derived (Michas et al. 2013):

$$P(>X) = \left[1 - (1-q)\frac{X}{X_o}\right]^{\frac{2-q}{1-q}}. \tag{2.1.13}$$

Another type of distributions that are deeply connected to statistical physics is that of the squared variable X^2. In BG statistical physics, the distribution of X^2 corresponds to the well-known Gaussian distribution. If we optimize S_q for X^2, we obtain a generalization of the normal Gaussian that is known as q-Gaussian distribution (see Tsallis 2009) and has the form:

$$p(X) = p_0\left[1 - (1-q)\left(\frac{X}{X_o}\right)^2\right]^{1/(1-q)}. \tag{2.1.14}$$

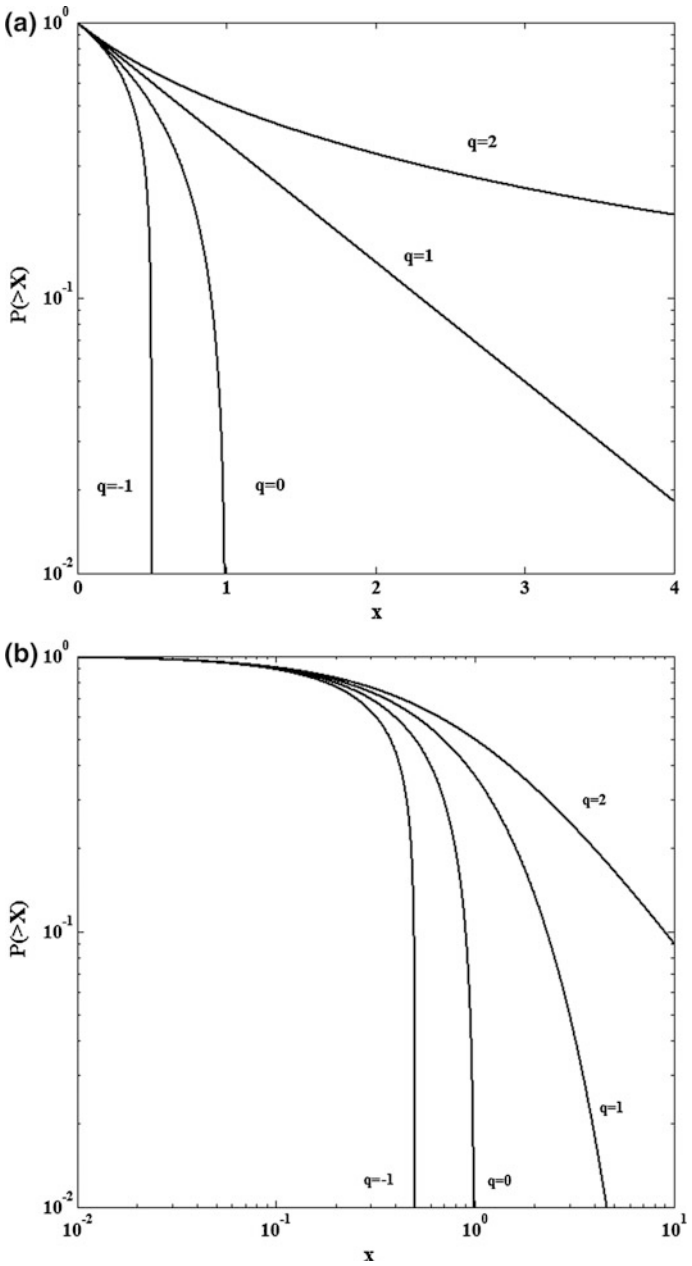

Fig. 1 The q-exponential distribution of Eq. (2.1.10) for various values of q and for $X_0 = 1$ in log-linear (**a**) and log-log scales (**b**). The distribution is convex for $q > 1$ and concave for $q < 1$. For $q < 1$, it has a vertical asymptote at $x = (1 - q)^{-1}$ and for $q > 1$ an asymptotic slope $-1/(q - 1)$. For $q = 1$ the standard exponential distribution is recovered

In the limit $q \rightarrow 1$, Eq. (2.1.14) recovers the normal Gaussian distribution. For $q > 1$, the q-Gaussian distribution has power-law tails with slope $-2/(q-1)$, thus enhancing the probability of the extreme values. Typical examples of q-Gaussians are plotted in Fig. 2 for various values of q.

2.2 Cases with Two Slopes

There are various cases in earthquake populations where the observed variable exhibits a distribution with different regions that correspond to different slopes. The most common example is gamma distribution that exhibits a power-law region for small and intermediate values and an exponential tail for greater values of the observed variable. This particular distribution has been used most frequently to model inter-event times (e.g. Corral 2004) and the global earthquake frequency-size distribution (e.g. Kagan 1997). In this latter case, an upper bound or taper in the G-R relation is appearing (Kagan and Jackson 2000) and the G-R relation is modified to include an exponential tail for modeling greater earthquake magnitudes. Estimating this upper bound or the correct distribution that corresponds to earthquake size distribution is of high importance in probabilistic earthquake hazard assessments (see for instance Kagan and Jackson 2013) and fundamental in constraining insurance risk for the largest events (Bell et al. 2013).

In the following we describe how distributions with crossovers and different behavior for large values of the observed variable can be derived in the frame of non-extensive statistical physics, by generalizing the physical probability given in Eq. (2.1.6).

The generalized probability $p(X)$ given by Eq. (2.1.6) can be alternatively obtained by solving the nonlinear differential equation:

$$\frac{dp}{dX} = -\beta_q p_i^q, \tag{2.2.1}$$

where $q \neq 1$; while Boltzmann-Gibbs (BG) formalism is approached in the limit $q \rightarrow 1$. We can now further generalize the standard representation of NESP, presented in the previous Sect. (2.1), by considering not only one q index, but a whole distribution of indices (see Tsallis et al. 1999; Tsekouras and Tsallis 2005). In the case where crossover to another type of behavior at larger values of the variable X is observed we can generalize the differential equation Eq. (2.2.1) as:

$$\frac{dp}{dX} = -\beta_r p^r - (\beta_q - \beta_r) p^q. \tag{2.2.2}$$

Equation (2.2.1) is recovered if $r = 0$ or if $r = q$. When $1 \leq r < q$, the solution of Eq. (2.2.2) is given by:

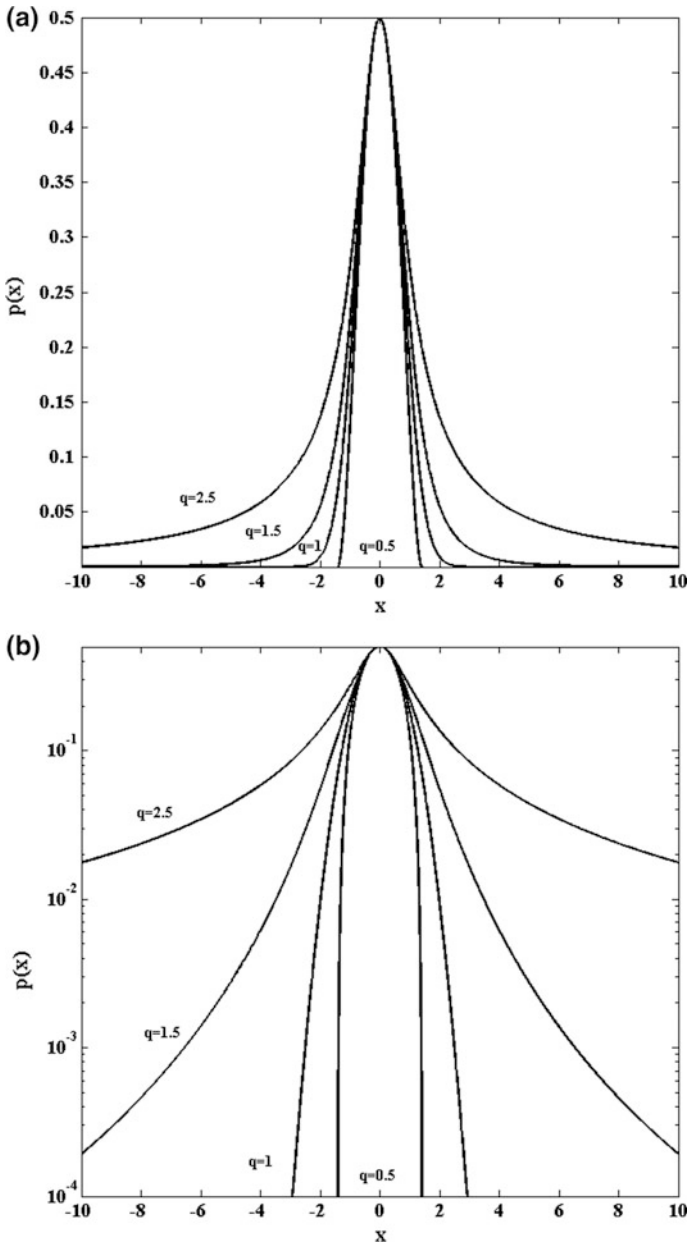

Fig. 2 The q-Gaussian distribution of Eq. (2.1.14) for various values of q and for $p_0 = 0.5$ and $X_0 = 1$ in linear (**a**) and log-linear scales (**b**). For $q = 1$ the normal Gaussian distribution is recovered

$$X = \int_{p}^{1} \frac{dx}{\beta_r x^r + (\beta_q - \beta_r)x^q} = \frac{1}{\beta_r} \int_{p}^{1} dx \left[\frac{1}{x^r} - \frac{\left(\frac{\beta_q}{\beta_r} - 1\right)x^{q-2r}}{1 + (\frac{\beta_q}{\beta_r} - 1)x^{q-r}} \right]$$

and hence

$$X = \frac{1}{\beta_r} \left\{ \frac{p^{-(r-1)} - 1}{r-1} - \frac{\frac{\beta_q}{\beta_r} - 1}{1 + q - 2r} \left[H\left(1; q-2r, q-r, \left(\beta_q/\beta_r\right) - 1\right) \right.\right. \\ \left.\left. - H\left(p; q-2r, q-r, \left(\beta_q/\beta_r\right) - 1\right) \right] \right\} \tag{2.2.3}$$

with

$$H(\xi; a, b, c) = \xi^{1+\alpha} F\left(\frac{1+a}{b}, 1; \frac{1+a+b}{c}; -\xi^b c\right) \tag{2.2.4}$$

where F is the hypergeometric function.

From the aforementioned solution of Eq. (2.2.2) for $1 \le r < q$ and $\beta_r << \beta_q$ the asymptotic solution defines three regions. The first one is related with very small values of the variable X and

$$p(X) \propto 1 - \beta_q X \quad \text{for } 0 \le X \le X_{c1}, \quad \text{where} \quad X_{c1} = \frac{1}{q-1}\frac{1}{\beta_q} \tag{2.2.5}$$

The second one describes the moderate values and

$$p(X) \propto [(q-1)\beta_q X]^{-1/(q-1)} \text{ for } X_{c1} \le X \le X_{c2}, \quad \text{where} \quad X_{c2} = \frac{[(q-1)\beta_q]^{\frac{r-1}{q-r}}}{[(r-1)\beta_r]^{\frac{q-1}{q-r}}}. \tag{2.2.6}$$

The third region describes the range of large values of X and

$$p(X) \propto [(r-1)\beta_r X]^{-1/(r-1)} \text{ for } \ge X_{c2}. \tag{2.2.7}$$

A special case of the differential Eq. (2.2.2) is when a crossover from anomalous ($q \neq 1$) to normal ($r = 1$) statistical mechanics is appearing for the larger values of the variable X (the truncated G-R relation for instance, described earlier). In this case, the differential equation Eq. (2.2.2) is modified as:

$$\frac{dp}{dX} = -\beta_1 p - (\beta_q - \beta_1)p^q \tag{2.2.8}$$

and includes both the normal and anomalous cases in the first and second term respectively. The solution of Eq. (2.2.8) is given by:

$$p = C\left[1 - \frac{\beta_q}{\beta_1} + \frac{\beta_q}{\beta_1} e^{(q-1)\beta_1 X}\right]^{-1/q-1} \tag{2.2.9}$$

were C is a normalization factor. For positive β_q and β_1, $p(X)$ decreases monotonically with increasing X (Vallianatos and Sammonds 2010). It can be easily verified that in the case where $\beta_q \gg \beta_1$ Eq. (2.2.9) defines again three regions, according to the value of X. The asymptotic behavior of the probability distributions in these areas, when $r = 1$, is simplified as

$$p(X) \propto 1 - \beta_q X \quad \text{for } 0 \le X \le X_{c1} \quad \text{where} \quad X_{c1} = \frac{1}{q-1}\frac{1}{\beta_q} \tag{2.2.10}$$

$$p(X) \propto [(q-1)\beta_q X]^{-1/(q-1)} \quad \text{for } X_{c1} \le X \le X_{c2} \quad \text{where} \quad X_{c2} = \frac{1}{[(q-1)\beta_1]} \tag{2.2.11}$$

$$p(X) \propto \left[\frac{\beta_1}{\beta_q}\right]^{-1/(q-1)} e^{-\beta_1 X} \quad \text{for } X \ge X_{c2} \tag{2.2.12}$$

where X_{c1} and X_{c2} are the lower and upper crossover points between the three regions respectively.

3 Applications in Seismicity

As already mentioned in the introduction of this chapter, seismicity and fault systems are among the most relevant paradigms of self-organized criticality (Bak et al. 1987, 2002), representing a complex spatiotemporal phenomenon (e.g. Telesca et al. 2001, 2002, 2003). Despite the complexity that characterizes fracturing and earthquake nucleation phenomena, simple phenomenology seems to apply in their collective properties, where empirical scaling relations are known to describe the statistical properties of the fracture/fault and earthquake populations in a variety of scales. The best known is the Gutenberg-Richter (G-R) scaling relation (Gutenberg and Richter 1944) that expresses fractal power-law dependence in the frequency of earthquakes with energy (seismic moment) E with E:

$$P(E) \sim E^{-B} \tag{3.1}$$

If we consider that the earthquake energy E is related to the magnitude M as $E \sim 10^{1.5M}$ (Kanamori 1978) and for $B = 1 + b/1.5$, the last expression can be

alternatively stated as $N(>M) \sim 10^{-bM}$, where $N(>M)$ is the number of earthquakes with magnitude equal or greater than M and b is a constant known as the seismic b-value.

Another well-known scaling relation is the modified Omori formula (Omori 1894; Utsu et al. 1995) where the aftershock production rate $n(t) = dN(t)/dt$ after main earthquakes decays as a power-law with time t:

$$n(t) = K(t + c)^{-p} \tag{3.2}$$

where K and c are constants that are determined from the data and p is the power-law exponent.

Power-laws and fractality have been also found in the space of earthquake locations and laboratory AE (Kagan and Knopoff 1980; Hirata and Imoto 1991) and at the time of their occurrence (Kagan and Jackson 1991; Turcotte 1997).

Crack and fault populations are characterized by scale-invariance so that their length distribution decays as a power-law:

$$N(>L) = AL^{-D} \tag{3.3}$$

where N is the number of faults with length equal or greater than L, A is a constant and D is the scaling exponent (Main 1996; Turcotte 1997).

The properties that are appearing in the earthquake and fault populations, such as those described above are the central subject in the statistical physics approach to seismicity. The necessity of statistical physics in deriving probability distributions for describing seismicity have been highlighted in the early works of Berrill and Davis (1980), Main and Burton (1984), where classic statistical physics and Shannon's information entropy (Shannon 1948) have been used to assess the probability of large earthquakes. Reviews for the classic statistical physics approach in seismicity can be found in Main (1996), Rundle et al. (2003) and Kawamura et al. (2012).

In the following sections we describe how appropriate probability distributions for the description of seismicity and the fault systems can be derived in the frame of NESP by using the maximum entropy principle and how these are applied to fracture and earthquake data, providing various examples for different case studies.

3.1 Non-extensive Pathways in Earthquake Size Distributions

3.1.1 The Fragment-Asperity Model

Earthquakes are originating from the deformation and sudden rupture of parts of the earth's brittle crust releasing energy and generating elastic waves that are propagating in the earth's interior. The generated waves are recorded in seismographic stations and properties such as the location and seismic moment of the earthquake

are calculated from the waveforms. Primarily, the earthquake generation process is a mechanical phenomenon where stick-slip frictional instability in pre-existing fault zones has a dominant role (e.g. Scholz 1998). Some well-known models, such as the spring-block model (Burridge and Knopoff 1967) and the cellular automaton model (Olami et al. 1992) have been developed to describe the phenomenology of this mechanism. In these models a stick-slip behavior in a set of moving blocks interconnected via elastic springs reproduce well some of the known empirical relations such as the Gutenberg-Richter (G-R) scaling law.

Consisted to the idea of stick-slip frictional instability in faults, Sotolongo-Costa and Posadas (2004) developed the fragment-asperity interaction model to describe earthquake dynamics in a non-extensive context. In this model, the triggering mechanism of an earthquake involves the interaction between the irregular surfaces of the fault planes and the fragments of various sizes and shapes that fill the space between them. When the accumulated stress exceeds a critical value in a particular fault zone, the fault planes are slipping, displacing the fragments and breaking possible asperities that hinder their motion, releasing energy (for an asperity based model for fault dynamics see De Rubeis et al. 1996). Sotolongo-Costa and Posadas considered that the released seismic energy is related to the size of the fragments and by using a non-extensive formalism they established an energy distribution function (EDF) for earthquakes based on the fragments-size distribution. Since the standard Boltzmann-Gibbs formalism cannot account for the presence of scaling in the fragmentation process, NESP seems more adequate to describe the phenomenon. The latter is also supported by the scale-invariant properties of fragments (Krajinovic and Van Mier 2000), the presence of long-range interactions among the fragmented materials (Sotolongo-Costa and Posadas 2004) and laboratory experiments in fracturing processes (Vallianatos et al. 2011, 2012a).

In the following we describe how the fragment-asperity model of Sotolongo-Costa and Posadas (2004), as was later revised by Silva et al. (2006) and Telesca (2012), is derived in the frame of NESP.

In terms of the probability $p(\sigma)$ of finding a fragment of area σ, the maximum Tsallis entropy S_q is expressed as:

$$S_q = k_B \frac{1 - \int p^q(\sigma)\, d\sigma}{q - 1}. \tag{3.1.1}$$

The sum of all the possible states in the definition of entropy is here expressed through the integration in all the sizes of the fragments. In what follows we set k_B equal to unity for the sake of simplicity. The probability $p(\sigma)$ is obtained after maximization of S_q under the appropriate two constraints. The first is the normalization of $p(\sigma)$:

$$\int_0^\infty p(\sigma) d\sigma = 1. \tag{3.1.2}$$

The second is the condition about the q-expectation value (Tsallis 2009):

$$\sigma_q = \langle \sigma \rangle_q = \frac{\int_0^\infty \sigma p^q(\sigma) d\sigma}{\int_0^\infty p^q(\sigma) d\sigma}. \tag{3.1.3}$$

This last condition reduces to the definition of the mean value in the limit $q \rightarrow 1$.

By using the Lagrange multipliers technique, the functional entropy to be maximized is (Silva et al. 2006):

$$\delta S_q^* = \delta \left(S_q + \alpha \int_0^\infty p(\sigma) d\sigma - \beta \sigma_q \right) = 0, \tag{3.1.4}$$

where α and β are the Lagrange multipliers. After some algebra, the following expression for the fragment size distribution function can be derived (Silva et al. 2006):

$$p(\sigma) = \left[1 - \frac{(1-q)}{(2-q)} (\sigma - \sigma_q) \right]^{1/(1-q)}. \tag{3.1.5}$$

The proportionality between the released relative energy E and the size of the fragments r is now introduced as $E \sim r^3$ (Silva et al. 2006), in accordance to the standard definition of seismic moment scaling with rupture length (Lay and Wallace 1995). The proportionality between the released relative energy E and the three-dimensional size of the fragments r^3 now becomes:

$$\sigma - \sigma_q = \left(\frac{E}{\alpha_E} \right)^{2/3}. \tag{3.1.6}$$

In the last equation, σ scales with r^2 and α_E is the proportionality constant between E and r^3 that has the dimension of volumetric energy density. By using the latter equation, the energy distribution function (EDF) of the earthquakes can be written on the base of the relationship between density functions of correlated stochastic variables (Telesca 2012):

$$p(E) = \frac{1}{\frac{dE}{d\sigma}} p \left[\left(\frac{E}{\alpha_E} \right)^{2/3} + \sigma_q \right] = \frac{d\sigma}{dE} \left[1 - \frac{(1-q)}{(2-q)} \left(\frac{E}{\alpha_E} \right)^{2/3} \right]^{\frac{1}{(1-q)}}, \tag{3.1.7}$$

where the term $d\sigma/dE$ can be obtained by differentiating Eq. (3.1.6):

$$\frac{d\sigma}{dE} = \frac{2}{3}\frac{E^{-\frac{1}{3}}}{\alpha_E^{\frac{2}{3}}} dE. \tag{3.1.8}$$

The EDF now becomes (Silva et al. 2006; Telesca 2012):

$$p(E) = \frac{C_1 E^{-\frac{1}{3}}}{\left[1 + C_2 E^{\frac{2}{3}}\right]^{1/(q-1)}}, \tag{3.1.9}$$

with $C_1 = \frac{2}{3\alpha_E^{\frac{2}{3}}}$ and $C_2 = \frac{(1-q)}{(2-q)\alpha_E^{\frac{2}{3}}}$.

In the latter expression, the probability of the energy is $p(E) = n(E)/N$, where $n(E)$ corresponds to the number of earthquakes with energy E and N is the total number of earthquakes. A more viable expression can now be obtained by introducing the normalized cumulative number of earthquakes given by the integral of Eq. (3.1.9):

$$\frac{N(E > E_{th})}{N} = \int_{E_{th}}^{\infty} p(E) dE, \tag{3.1.10}$$

where $N(E > E_{th})$ is the number of earthquakes with energy E greater than the threshold energy E_{th} and N the total number of earthquakes. Substituting Eq. (3.1.9) in Eq. (3.1.10) the following expression is derived:

$$\frac{N(E > E_{th})}{N} = \left[1 - \left(\frac{1 - q_E}{2 - q_E}\right)\left(\frac{E}{\alpha_E}\right)\right]^{\frac{2-q_E}{1-q_E}}. \tag{3.1.11}$$

Now the latter expression can be written in terms of the earthquake magnitude M, if we consider that E is related to M as $M = \frac{2}{3}\log(E)$ (Kanamori 1978). Then Eq. (3.1.11) becomes:

$$\frac{N(>M)}{N} = \left[1 - \left(\frac{1 - q_E}{2 - q_E}\right)\left(\frac{10^M}{\alpha_E^{2/3}}\right)\right]^{\frac{2-q_E}{1-q_E}}. \tag{3.1.12}$$

In real earthquake catalogues the threshold magnitude M_0, i.e. the minimum magnitude M_0 of the catalogue, has to be taken in account and Eq. (3.1.12) should be slightly changed to (Telesca 2012):

$$\frac{N(>M)}{N} = \left[\frac{1-\left(\frac{1-q_E}{2-q_E}\right)\left(\frac{10^M}{\alpha_E^{2/3}}\right)}{1-\left(\frac{1-q_E}{2-q_E}\right)\left(\frac{10^{M_0}}{\alpha_E^{2/3}}\right)}\right]^{\frac{2-q_E}{1-q_E}}. \quad (3.1.13)$$

The fragment-asperity model describes from the first principles the cumulative distribution of the number of earthquakes N greater than a threshold magnitude M, normalized by the total number of earthquakes. The constant a_E expresses the proportionality between the released energy and the fragments of size r, while q_E is the entropic index. This model has been recently applied to various regional earthquake catalogs, covering diverse tectonic regions (Silva et al. 2006; Vilar et al. 2007; Telesca 2010a, b, c, 2011; Michas et al. 2013; Papadakis et al. 2013) and volcano related seismicity (Telesca 2010b; Vallianatos et al. 2013). In comparison to the G-R scaling relation (Eq. 3.1), the fragment-asperity model describes appropriately the energy distribution in a wider range of magnitudes, while for values above some threshold magnitude, the G-R relation can be deduced as a particular case for $b = (2 - q_E)/(q_E - 1)$ (Telesca 2012).

Some relevant paradigms for the application of the fragment—asperity model to earthquake data are given in Figs. 3, 4 and 5. In Fig. 3 the model is applied to the energy distribution function of earthquakes in the West Corinth rift (Greece), according to Eq. (3.1.9). In this case the model describes better than the G-R relation (Eq. 3.1) the observed distribution for the lower earthquake energies, while after some threshold energy the distribution decays as a power-law (Michas et al. 2013). Another example comes from the recent unrest at the Santorini volcanic complex (Vallianatos et al. 2013), where the normalized cumulative magnitude distribution of the volcano seismicity is well described by the model (Eq. 3.1.12) for the value of the entropic index $q_E = 1.39$ (Fig. 4).

The entropic index q_E has been recently used by Papadakis et al. (2013) to geodynamically characterize various seismic zones along the Hellenic Subduction Zone (HSZ). Figure 5 shows the distribution of the relative cumulative number of

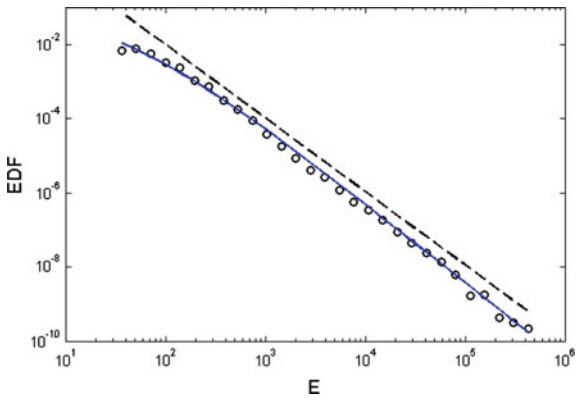

Fig. 3 The energy distribution function (*circles*) and the fitted curve (*solid line*). The *dashed line* represents the G-R relation for $b = 1.51 \pm 0.03$ (Michas et al. 2013)

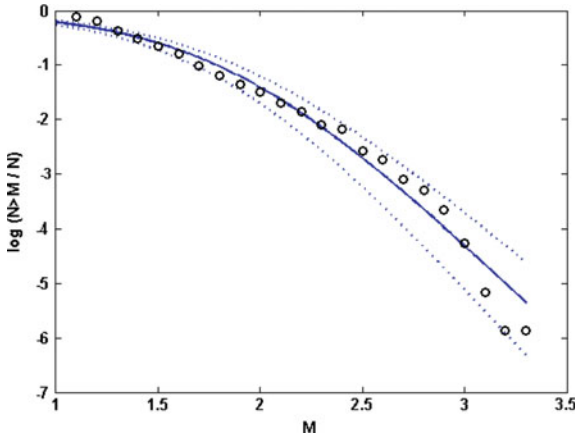

Fig. 4 Normalized cumulative magnitude distribution of the Santorini seismicity (*circles*) and the fitting curve (*solid line*). The values for the best fit regression to the data are $q_E = 1.39 \pm 0.035$ and $a = 286.6 \pm 78$. The 95 % confidence intervals for q_E and a are also plotted (*dashed lines*) (Vallianatos et al. 2013)

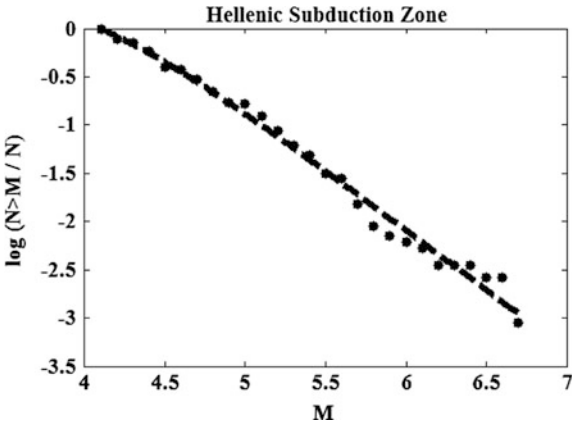

Fig. 5 The *black dashed line* indicates the non-extensive fitting curve for the HSZ as a unified system (Papadakis et al. 2013)

earthquakes as a function of magnitude M for the Hellenic Subduction Zone as a unified system and the fitting according to the model of Eq. (3.1.13), while Fig. 6 shows the variation of the q_E value along the HSZ, where the variation is related to the energy release rate in each seismic zone.

3.1.2 Global Earthquake Size Distribution. The Effect of Mega-Earthquakes

The global earthquake frequency-magnitude distribution is among the long-standing statistical relationships of seismology. Recently, Vallianatos and

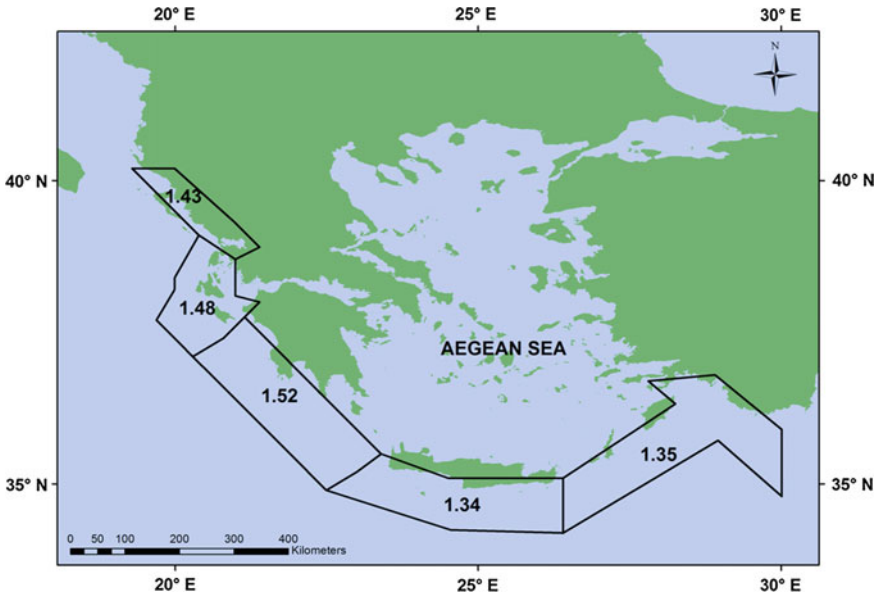

Fig. 6 The variation of the q_E value along the seismic zones of the HSZ (Papadakis et al. 2013)

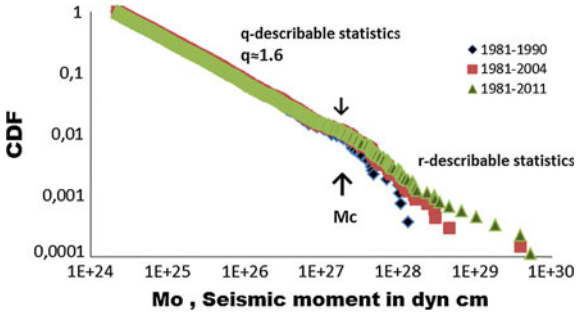

Fig. 7 Distribution of seismicity versus seismic moment for the centroid moment tensor catalogue up to the end of 1990 (before Sumatra mega event, in *black*), the end of December 2004 (after Sumatra, in *red*) and within a week after Honshu mega earthquake (till 17 March 2011, in *green*), for shallow events ($H < 75$ km), with $M_w > 5.5$, since 1 January 1981. This is plotted as a normalized cumulative distribution function (*CDF*) against seismic moment (Vallianatos and Sammonds 2013)

Sammonds (2013) used non-extensive statistical mechanics to characterize the global earthquake frequency–magnitude distribution and to interpret observations from the Sumatran and Honshu earthquakes. Examples of the cumulative distribution function (CDF) from the CMT seismic moment M_o data are given in Fig. 7.

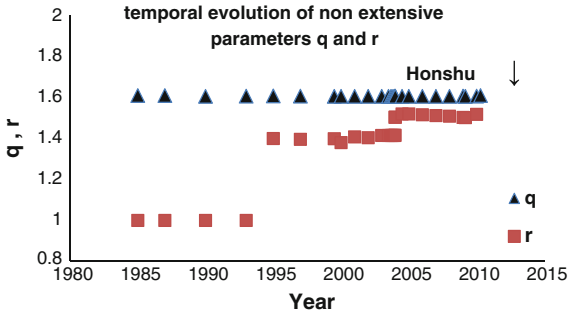

Fig. 8 Temporal evolution of non-extensive parameters q and r extracted from the analyses of seismic moment distribution using the global CMT catalogue. We observe a stable organization in moderate events in contrast to a significant change of r, which supports the concept of the global organization of seismicity before the two recent Sumatra and Honshu mega events (Vallianatos and Sammons 2013)

The aforementioned authors found that global seismicity is described by non-extensive statistical mechanics and that the seismic moment distribution reflects a sub-extensive system, where long-range interactions are important.

Using the cross-over formulation of non-extensive statistical physics (see Sect. 2.2), Vallianatos and Sammonds (2013) conclude that the seismic moment distribution of moderate events yields thermodynamic q-values of $q_E = 1.6$ which seem to be constant for the duration of the Sumatra and Honshu earthquake preparation, while r_M (which describes the seismic moment distribution of great events) varies from 1 that corresponds to an exponential function (Eqs. 2.2.8–2.2.12), to 1.5 and another power-law regime (Eqs. 2.2.2–2.2.7) as we approach the mega events (Fig. 8).

3.1.3 Increments of Earthquake Energies

The probability distribution in the incremental earthquake energies is referred to the probability that an earthquake of energy $S(i)$ will be followed by one with energy $S(i + 1)$ with difference R, expressed as $R = S(i + 1) - S(i)$ ($i = 1, 2, \ldots, N - 1$ where N the total number). Caruso et al. (2007) have calculated this probability for a dissipative Olami–Feder–Christensen model (OFC—Olami et al. 1992) and showed that in the critical regime (small-world lattice) the probability distribution $P(R)$ follows a q-Gaussian, while in the noncritical regime (regular lattice) the distribution $P(R)$ is close to a Gaussian distribution. Then considering the quantity $S = \exp(M)$ as a measure of the energy S of an earthquake of magnitude M, Caruso et al. (2007) showed that the probability distribution $P(R)$ for real earthquakes in Northern California and in the entire world follows a q-Gaussian distribution as well, providing further evidence for self-organized criticality, intermittency and long-range interactions in seismicity.

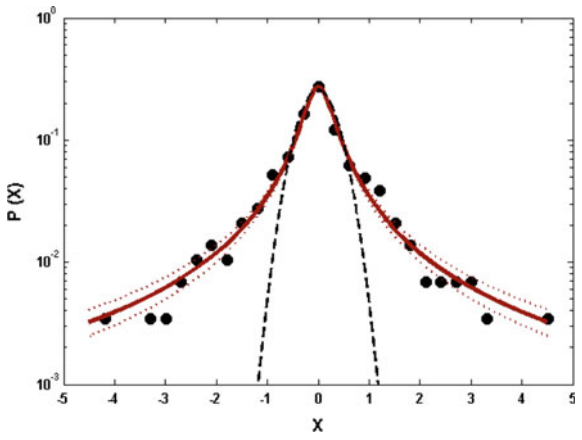

Fig. 9 Probability density function $P(X)$ (*solid circles*) for the 2011–2012 earthquake activity in Santorini volcanic complex on a semi-log plot, where $S = \exp(M)$, $R = S(i + 1) - S(i)$, $X = (R - \langle R \rangle)/\sigma_R$ and $\langle R \rangle$ the mean and σ_R the standard deviation. The *dashed curve* represents the standard Gaussian shape. The data is well fitted by a q-Gaussian curve (*solid line*) for the value of the entropic index $q_R = 2.24 \pm 0.09$ (95 % confidence intervals—*dotted curves*) (Vallianatos et al. 2013)

In addition, Vallianatos et al. (2013) studied the probability distribution of incremental energies in the volcano related seismicity during the 2011–2012 unrest at the Santorini volcanic complex. The probability density function of R, normalized to zero mean and unit variance and subjected to the normalization condition $\int p(R)dR = 1$ exhibits fat tails and can be well described by a q-Gaussian distribution (Eq. 2.1.14) for the value of $q = 2.24 \pm 0.09$ (Fig. 9), indicating non-linear dynamics and self-organized criticality in the observed volcano-related seismicity. Here we provide further evidence by considering the global earthquakes with magnitude $M \geq 7$ that occurred during the period 1900–2012, as these are reported in the latest version of the Centennial earthquake catalog (Engdahl and Villaseñor 2002) (catalog available at http://earthquake.usgs.gov/data/centennial/) and supplemented by the ANSS earthquake catalog (http://www.ncedc.org/anss/) for the period 2007–2012. The probability density of the incremental earthquake energies exhibits fat tails and deviates from the normal Gaussian distribution (Fig. 10). A q-Gaussian distribution with $q = 1.85 \pm 0.1$ can well describe the observed distribution, thus enhancing the probability of large differences in the energies of successive earthquakes in global scale.

3.2 Spatiotemporal Description

Throughout the text we referred to the scale-invariant spatiotemporal properties of seismicity. Considering these properties, Abe and Suzuki proposed that the 3-dimensional hypocentral distances and the time intervals between the successive

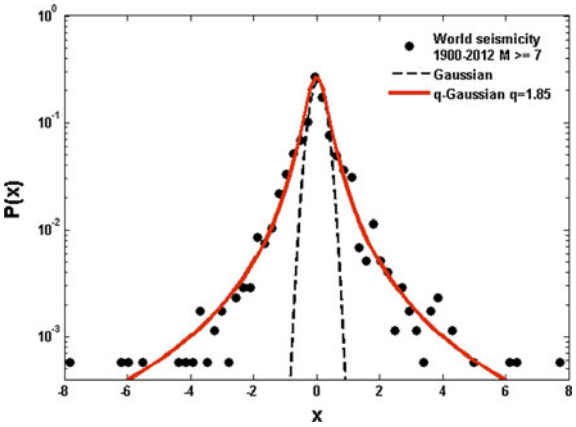

Fig. 10 Probability density function $P(X)$ (*solid circles*) for the 1900–2012 global seismicity with magnitude $M \geq 7$ on a semi-log plot, where $S = \exp(M)$, $R = S(i + 1) - S(i)$, $X = (R - \langle R \rangle)/\sigma_R$ and $\langle R \rangle$ the mean and σ_R the standard deviation. The normalization condition $\int p(R)dR = 1$ applies. The *dashed curve* represents the standard Gaussian shape and the *solid line* the q-Gaussian distribution for the value of $q = 1.85 \pm 0.1$

earthquakes follow a q-exponential distribution (see Sect. 2.1) with $q < 1$ and $q > 1$ respectively and verified their approach for the cumulative distribution of inter-event distances and times of successive earthquakes in California and Japan (Abe and Suzuki 2003, 2005). Since then, this approach has been successfully applied in various studies, covering diverse scales and tectonic regimes (e.g., Darooneh and Dadashinia 2008; Vallianatos et al. 2012a, b; Vallianatos and Sammonds 2013; Papadakis et al. 2013).

Such examples of the non-extensive statistical physics application to the spatiotemporal distributions of earthquakes for regional tectonics and mega-structure geodynamics are given in Figs. 11, 12, 13, 14, 15, 16, 17 and 18. In particular, in Fig. 11 the cumulative inter-event time distribution $P(>\tau)$ for the 1995 Aigion earthquake aftershock sequence is presented that follows a q-exponential distribution for $q_\tau = 1.58$ (Vallianatos et al. 2012b).

Papadakis et al. (2013) estimated the cumulative distribution functions of the inter-event times and distances along the HSZ (Figs. 12 and 13). Figures 14 and 15 show the variation of the calculated q_T and q_D values along the seismic zones of the HSZ. With the exception of seismic zone 4, which is located in the central part of the HSZ and covers the southern area of Crete, the q_T values appear close to each other while the q_D values seem to differ significantly. The latter result possibly reflects the fact that q_T is related with the time evolution of seismicity, which is a long term process in the Hellenic arc, with the highest temporal clustering in the area south of Crete. In addition the q_D variations indicate a different degree of spatial earthquake clustering along the seismic zones.

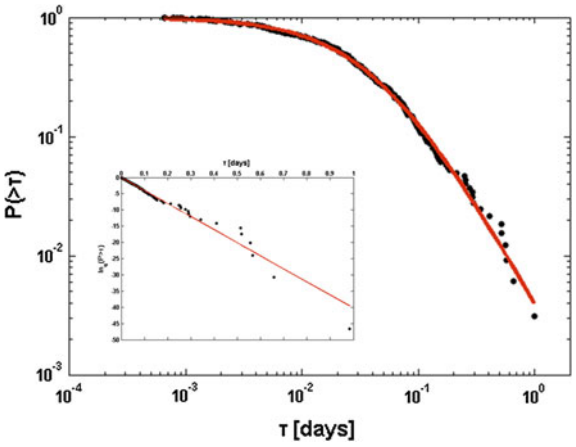

Fig. 11 Log-log plot of P(>τ). The *solid line* represents the q_τ-exponential distribution for the values of $q_\tau = 1.58 \pm 0.02$ and $\tau_0 = 0.025 \pm 0.0003$ days. *Inset* the q_τ-logarithmic distribution $\ln_q(P(>\tau))$, exhibiting a correlation coefficient of $r = -0.9885$. The *straight line* corresponds to the q-exponential distribution (Vallianatos et al. 2012b)

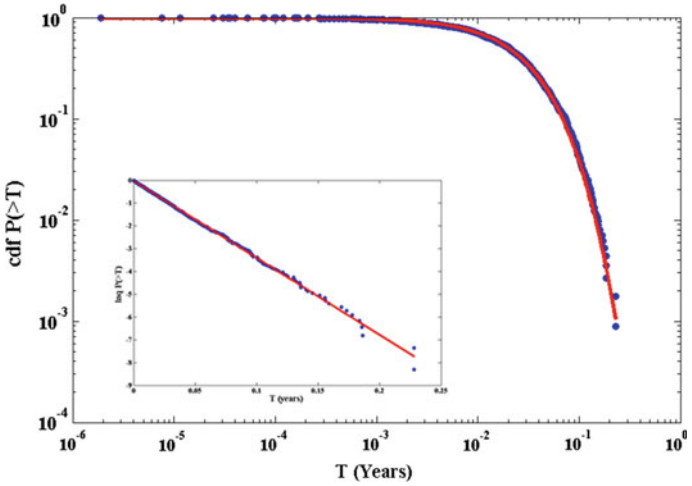

Fig. 12 The log-log plot of the inter-event times cumulative distribution for the HSZ as a unified system. *Inset* the semi-q-log plot of the inter-event times cumulative distribution for the HSZ as a unified system. The *dashed line* represents the q-logarithmic function (Papadakis et al. 2013)

Additionally, Vallianatos and Sammonds (2013), using global shallow seismicity with $M_w > 5.5$ extracted from CMT catalogue, analyzed the inter-event time distribution before and after the Sumatran and Honshu mega earthquakes. Figure 16 shows the inter-event times cumulative probability distribution $P(>\tau)$ and demonstrates that, in spite of the changes observed in non-extensive frequency-seismic

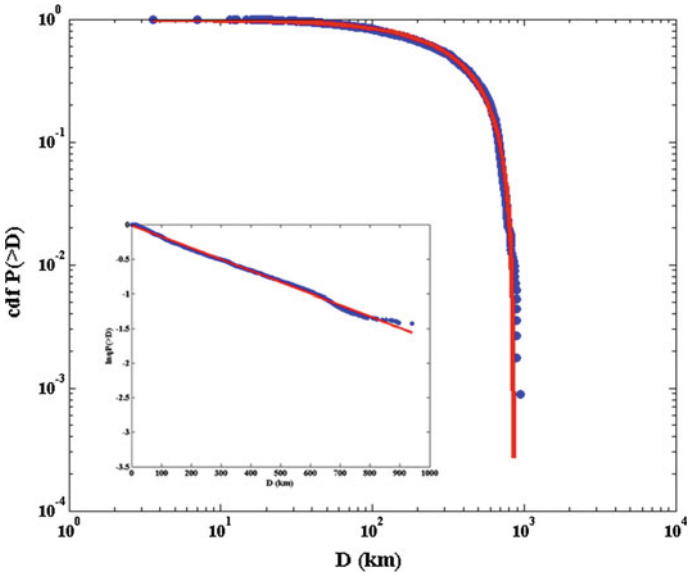

Fig. 13 The log-log plot of the three-dimensional distances cumulative distribution for the HSZ as a unified system. *Inset* The semi-q-log plot of the inter-event distances cumulative distribution for the HSZ as a unified system. The *dashed line* represents the q-logarithmic function (Papadakis et al. 2013)

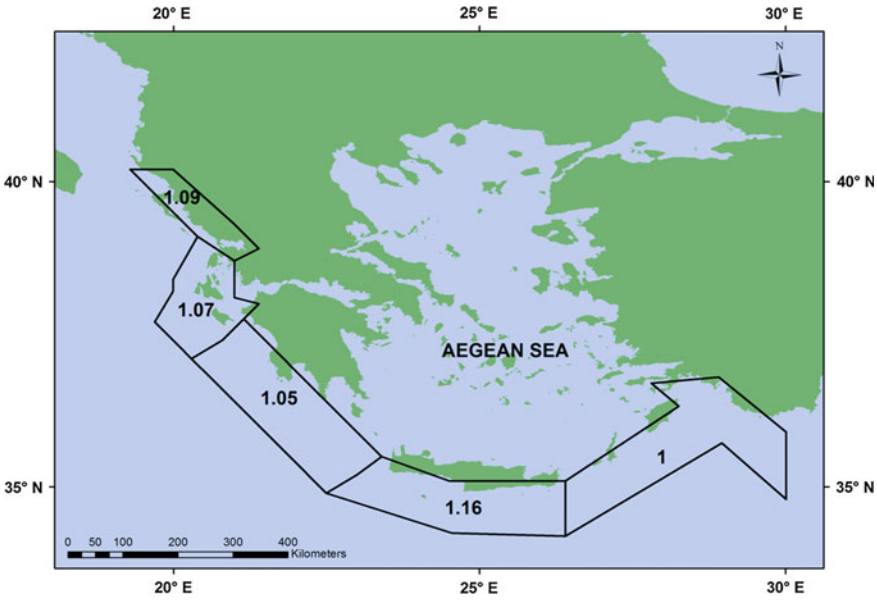

Fig. 14 The q_T variation along the HZS (Papadakis et al. 2013)

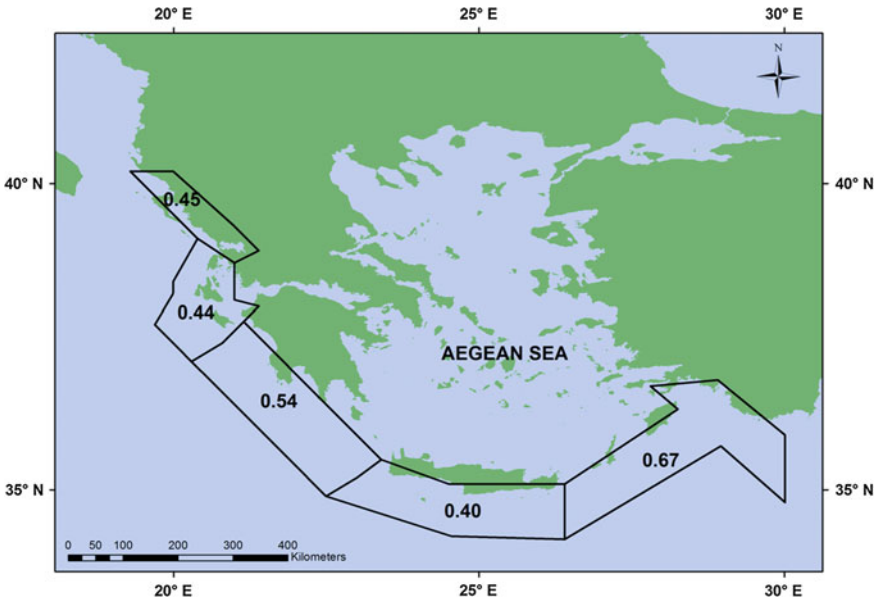

Fig. 15 The q_D variation along the HSZ (Papadakis et al. 2013)

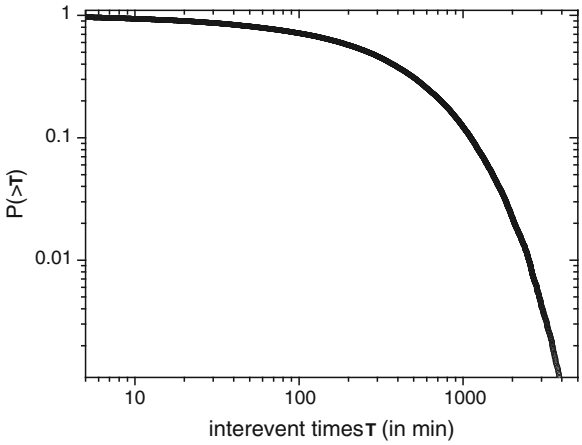

Fig. 16 Log-log plot of the cumulative distribution of inter-event times for the centroid moment tensor catalogue summed from 1.1.1981 to 31.12.2000, to 31.12.2005 and 27.03.2011 for shallow events $M_w > 5.5$. There is no change observed due to the Sumatran and Honshu earthquakes. The best fit regression is realized by $q_\tau = 1.52$ and $\tau_o = 290$ min. The associated value of the correlation coefficient between the data and the model is 0.99354 (Vallianatos and Sammonds 2013)

moment distribution, there is no change in global temporal distribution due to the mega earthquakes. Moreover the inter-event distances cumulative probability distribution $P(>D)$ (Fig. 17) does not present any change before and after mega-earthquakes.

Along with the cumulative inter-event time distribution, the probability distribution function of the normalized inter-event times of earthquakes in the West Corinth rift has been studied by Michas et al. (2013). In this case, inter-event times τ (in seconds) are scaled to the mean inter-event time $\bar{\tau} = (t_N - t_1)/(N-1)$ as $\tau' = \tau/\bar{\tau}$. For various threshold magnitudes, the probability distribution function exhibits two-power law regions for short and long inter-event times, indicating the presence of scaling and clustering at both short and long time scales (Fig. 18). This behavior can be well reproduced by a q-generalized gamma distribution (Queiros 2005) that has the form:

$$p(\tau\prime) = C\tau\prime^{(\gamma-1)} \exp_q(-\tau\prime/\theta), \tag{3.2.1}$$

where C, γ and θ are constants and $e_q(x)$ the q-exponential function (Eq. 2.1.7). In the limit $q \rightarrow 1$, Eq. (3.1) recovers the ordinary gamma distribution. This result indicate that short and intermediate inter-event times, directly related to the production of aftershock sequences, scale with exponent $\gamma - 1$ and long-inter-event times scale with exponent $1/(1-q)$.

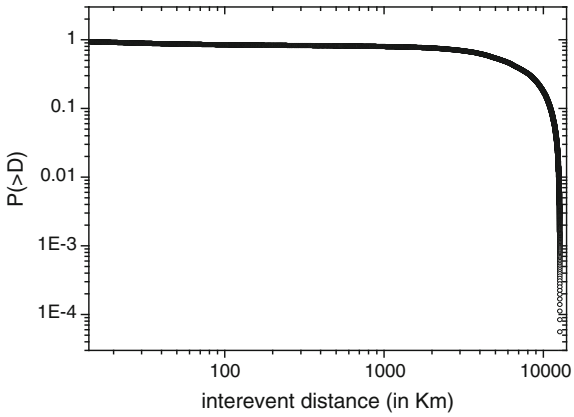

Fig. 17 Log-log plot of the cumulative distribution of inter-event distances for the centroid moment tensor catalogue summed from 1.1.1981 to 31.12.2000, to 31.12.2005 and 27.03.2011 for shallow events $M_w > 5.5$. There is no change observed due to the Sumatran and Honshu earthquakes. The best fit regression is realized by $q_D = 0.29$ and $D_o = 10^4$ km. The associated value of the correlation coefficient between the data and the model is 0.96889 (Vallianatos and Sammonds 2013)

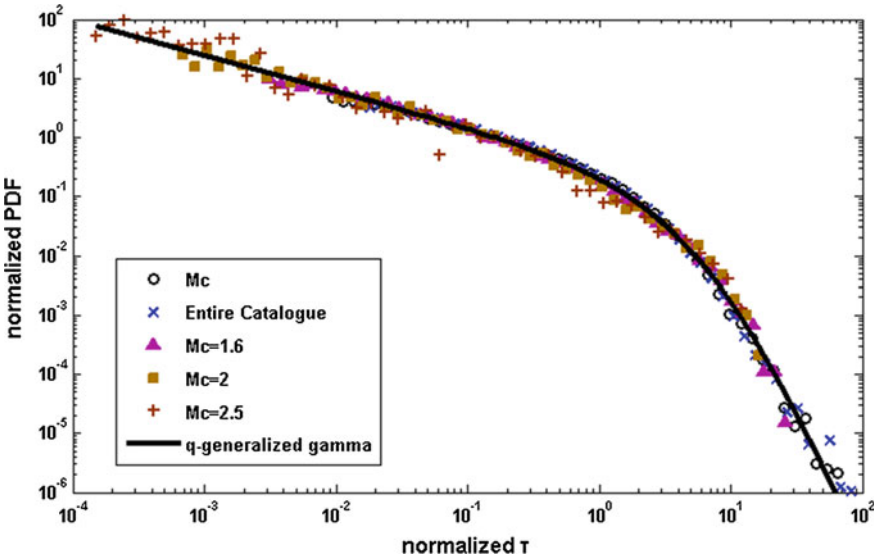

Fig. 18 Normalized probability density p (τ') for the scaled inter-event times τ' for various threshold magnitudes. *Solid line* represents the q-generalized gamma distribution (Eq. 3.2.1) for the values of $C = 0.35$, $\gamma = 0.39$, $\theta = 1.55$ and $q = 1.23$ (Michas et al. 2013)

3.3 *Fault Networks*

Fault systems have been documented on nearly every geologic surface in the solar system (Schultz et al. 2010) and represent a complex scale-invariant network of fractures and faults that is related morphologically and mechanically with the planetary lithosphere deformation and seismicity (Schultz 2003; Knapmeyers et al. 2006). In the last decades, innovative insights into the origin of fault population dynamics have been presented from the point of view of non-equilibrium thermodynamics (Prigogine 1980), fractal geometry (Mandelbrot 1983; Scholz and Mandelbrot 1989), thermodynamics of chaotic systems (Beck and Schlogl 1993) and complexity (Tsallis 2001, 2009).

Vallianatos et al. (2011b) and Vallianatos (2013) used non-extensive statistical physics to explore the distribution of the fault lengths. The aforementioned authors tested the applicability of non-extensive statistical physics in two extreme cases: (a) Crete, in the front of the Hellenic arc and (b) the fault distribution in an extraterrestrial planet, the Mars.

Fault lengths distributions in Central Crete presented by Vallianatos et al. (2011b) (Fig. 19) in the form of log-log plot of the cumulative distribution function (CDF) $P_{\mathrm{cum}}(>L)$ of the fault lengths. An analysis of the faults of Central Crete as a single set based on q-exponential distribution leads to $q = 1.16$.

We proceed now to explore using the principles of non-extensive statistical mechanics the fault population statistics derived for an extraterrestrial data set

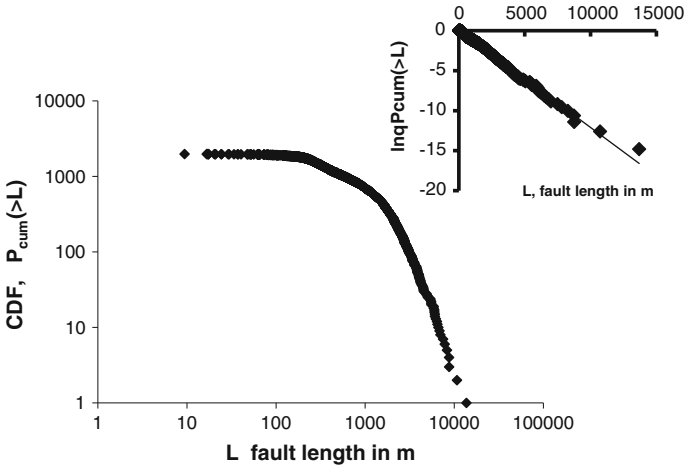

Fig. 19 Unormalized empirical CDF for all fault lengths in Central Crete graben. In the *upper right corner* the semi-q-log plot of the cumulative distribution function CDF of fault lengths for all the examined sets of Central Crete graben is presented (Vallianatos et al. 2011b)

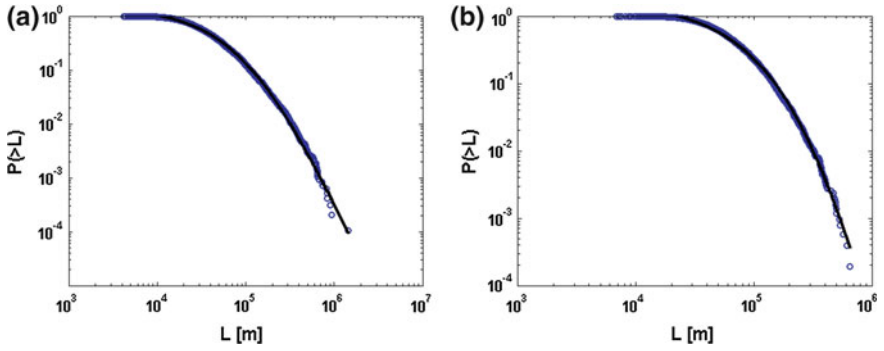

Fig. 20 The normalized cumulative distribution function $P(>L)$ for Mars **a** compressional and **b** extensional faults. The *black line* is the q-exponential fitting for **a** $q_c = 1.114$ for the trust (compressional) faults and **b** $q_e = 1.277$ for the normal (extensional) ones (Vallianatos 2013)

selected in a well-studied planet as Mars is. The Valles Marineris Extensional Province on Mars (Lucchitta et al. 1992; Mège and Masson 1996; Schultz 1995, 1997) includes perhaps the largest planetary rift-like structure in the solar system.

The cumulative distribution functions of faults (CDF) $P(>L)$, are shown as log-log plots in Fig. 20 for the cases of normal and thrust faults. The analysis of fault lengths in Mars indicates that $q_e = 1.277$ for the extensional (normal) faults, while $q_c = 1.114$ for the compressional (thrust) faults.

The q-values estimated supports the conclusion that the planetary fault system in Mars is a sub-additive one in agreement with a recent result (Vallianatos and

Sammonds 2011) for the Valles Marineris extensional province, Mars and for the regional fault structure in the front of the Hellenic arc (Vallianatos et al. 2011b), with consistency with that observed in local and global seismicity (Vallianatos and Sammonds. 2013; Vallianatos et al. 2013).

3.4 Plate Tectonics as a Case of Non-extensive Thermodynamics

In 2003, Bird presented a new global set of present plate boundaries on the Earth (in digital form) and proposed that the distribution of areas of the tectonic plates follows a power law and that this distribution fitted well with the concepts of a few major plates and a hierarchical self-similar organization of blocks at the boundary scale, a fractal plate distribution and a self-organized system.

Vallianatos and Sammonds (2010) applied the concept of non-extensive statistical mechanics to plate tectonics. The aforementioned authors calculated the probability density function for the areas of the tectonic plates. Figure 21 shows the complementary cumulative number $F(>A)$ of plates as a function of area A in steradians, i.e., the number of plates with an area equal to or larger than A. The data are accounted for by the power law, $F(>A) \propto A^{-\mu}$ with μ close to 1/3 except for the three smallest ranks and the largest plates. The results show that three classes (small, intermediate and large) of tectonic plates can be distinguished, which is consistent with the observations of Bird (2003). Vallianatos and Sammonds used the differential equation $dp_i/dA_i = -\beta_1 p_i - (\beta_q - \beta_1)p_i^q$ (see Sect. 2.2 "Cases with two slopes") in order to further generalize the anomalous equilibrium distribution, in such a way as to have a crossover from anomalous ($q \neq 1$) to normal ($q = 1$) statistical mechanics, while increasing the plate's area. From a visual inspection of Fig. 21, it might be argued that the deviation from the power law region occurs earlier at the seven largest plates with area more than 1 steradian and belong to a different population than the rest of the plates, indicating that a cross-over exist at $A_{c2} \approx 1$ steradian. Furthermore at the five smallest plates another cross-over exists at $A_{c1} \approx 3 \times 10^{-3}$steradians.

Taking into account that for the intermediate class of tectonic plates the cumulative frequency distribution behaves as a power law with exponent 1/3, the thermodynamic q parameter is calculated equal to $q = 1.75$, which supports the conclusion that the plate tectonics system is a sub-extensive one.

3.5 Laboratory Seismology

Recently, the statistical properties of fracture have attracted a wide interest in the statistical physics community (Herrmann and Roux 1990; Chakrabarti and Benguigui 1997). In this context, fracture can be seen as the outcome of the

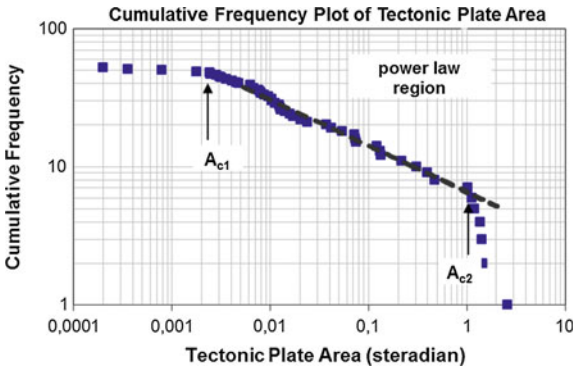

Fig. 21 Complementary cumulative distribution of the areas of tectonic plates compared to the fit with a power law (central long-*dashed line*) with exponent $\mu = 1/3$ (Vallianatos and Sammonds 2010)

irreversible dynamics of a long-range interacting, disordered system. Several experimental observations have revealed that fracture is a complex phenomenon, described by scale invariant laws (Krajcinovic and Van Mier 2000). Examples notably include the acoustic emission (AE) measured prior to fracture and the roughness of the fracture surface (Lei et al. 1992, 2000; and references therein).

Vallianatos et al. (2012a) investigated the statistical physics of fracture in a heterogeneous brittle material (Etna basalt) under triaxial deformation, analyzing the temporal and three dimensional location of moment release of acoustic emissions from micro-fractures that occur before the final fracture.

Using the calculated AE moment, the cumulative distribution function (CDF) $P(>M)$ of the AE scalar moments is shown in Fig. 22a, b presents the log-log plot of the cumulative distribution function $P(>T)$ of the AE inter-event times while Fig. 22c the log-log plot of the cumulative distribution function $P(>D)$ of the AE inter-event Euclidean distances.

The aforementioned authors showed that the scalar moment distribution and the inter-event time distribution of AE, are expressed by the non-extensive statistical mechanics of a sub-additive process with q-values $q_M = 1.82$ and $q_\tau = 1.34$ respectively supporting the idea of the presence of long-range effects. The inter-event distances described by q-statistics with $q_D = 0.65$. The above suggests that AEs in Etna's basalt are described by the q-value triplet $(q_M, q_\tau, q_D) = (1.82, 1.34, 0.65)$. Furthermore, it should be noticed that the sum of q_τ and q_D indices of the distribution of the inter-event time and distance is $q_\tau + q_D \approx 2$, similar with that observed in regional seismicity data both from Japan and California (Abe and Suzuki 2003, 2005) and verified numerically using the two dimensional Burridge-Knoppoff model (Hasumi 2007, 2009). These results indicate that AEs exhibits a non-extensive spatiotemporal duality similar with that observed with earth seismicity (Abe and Suzuki 2003, 2005; Vallianatos 2009; Vallianatos and Sammonds 2011).

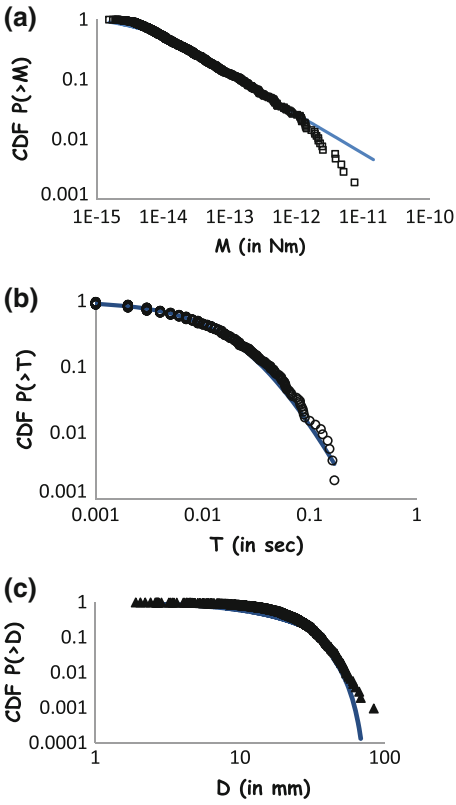

Fig. 22 **a** The cumulative distribution function (*CDF*), $P(>M)$ of the AEs scalar moment M, along with the q-exponential fitting curve. **b** The cumulative distribution function $P(>T)$ of the AEs inter-event time T, along with the q-exponential fitting curve. **c** The cumulative distribution function $P(>D)$ of the AEs inter-event Euclidean distance D, along with the q-exponential fitting curve (Vallianatos and Triantis 2012a)

3.6 *Can Non-extensive Statistical Physics Predict Seismicity's Evolution?*

Recently, the ideas of non-extensive statistical physics have been used to uncover hidden dynamic features of seismicity before strong events (Papadakis et al. 2014; Vallianatos et al. 2014). These studies examine possible variations of the thermo-statistical parameter q_E before the occurrence of a mainshock. This parameter, which is derived from the fragment asperity model (Sotolongo-Costa and Posadas, 2004), is related to the frequency-magnitude distribution and can be used as an index of the stability of a seismic area. The observed variations are consistent with the evolution of seismicity and seem a very useful tool for the distinction of different dynamical regimes towards a strong earthquake. It should be noticed that this approach has been applied to the strong event of L'Aquila, on April 6, 2009 (M_L = 5.8) (Telesca 2010c). The aforementioned author calculated an increase of the non-extensive parameter in a time interval starting some days before the occurrence of the mainshock.

Vallianatos et al. (2014) applied the concept of non-extensive statistical physics along with the method of natural time analysis (Varotsos et al. 2011) to examine the precursory seismicity of the Mw6.4, October 12, 2013 earthquake in the south-western part of the Hellenic Arc (Fig. 23). Varotsos et al. (2001), proposed the natural time analysis of a complex system, from which we deduce the maximum information from a given time series and we identify the time as we approach towards the occurrence of the mainshock (Varotsos et al. 2011).

Figure 24 presents the temporal evolution of the parameter q_E over increasing (cumulative) time windows. The initial time window has a 100-event width and increases per 1 event over time. The obtained q_E values are associated with the last event included in the window.

The analysis of the frequency-magnitude distribution according to Eq. (3.1.13) reveals that the non-extensive parameter q_E varies during the last period of the earthquake preparatory phase and exhibits a sharp increase a couple of days before the occurrence of the mainshock, indicating an increase in the degree of out-of-equilibrium state before the occurrence of the Mw6.4 earthquake.

Moreover, Papadakis et al. (2014) used the non-extensive formalism to decode the evolution of seismicity towards the January 17, 1995 Kobe earthquake (M = 7.2), in the southwestern part of Japan.

For the detection of possible variations of the non-extensive parameter q_E, the aforementioned authors calculated these variations in different time windows. Figure 25 shows the variations of q_E values over 200-event moving windows (overlapping), having a sliding factor equal to 1. The q_E parameter increases significantly on April 9, 1994 and peaks (q_E = 1.55) as we move towards the 1995

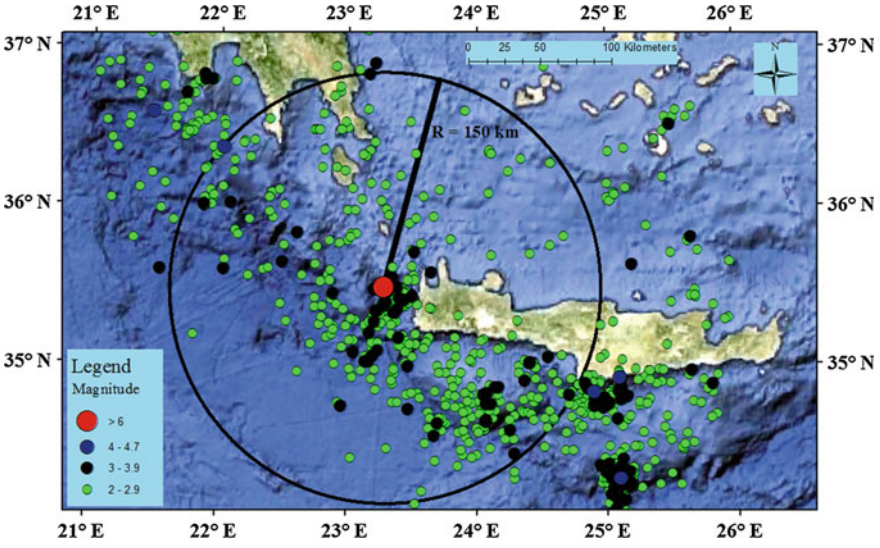

Fig. 23 The observed seismicity in the southwestern segment of the Hellenic Arc during the period 1 July–30 October, 2013

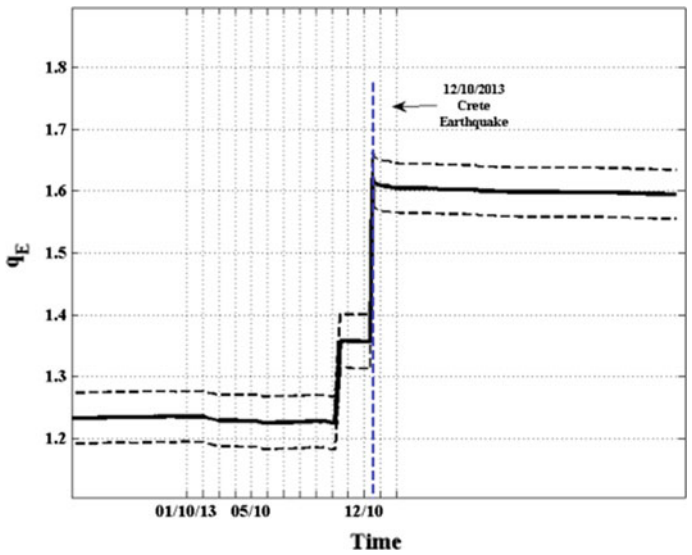

Fig. 24 The temporal evolution of the non-extensive parameter q_E for a circle area with radius R = 150 km around the epicenter of the main event. We note a sharp increase of q_E to the value $q_E \approx 1.36$ a couple of days before the occurrence of the strongest event, while a $q_E \approx 1.6$ is estimated immediately with the Mw6.4 strong event

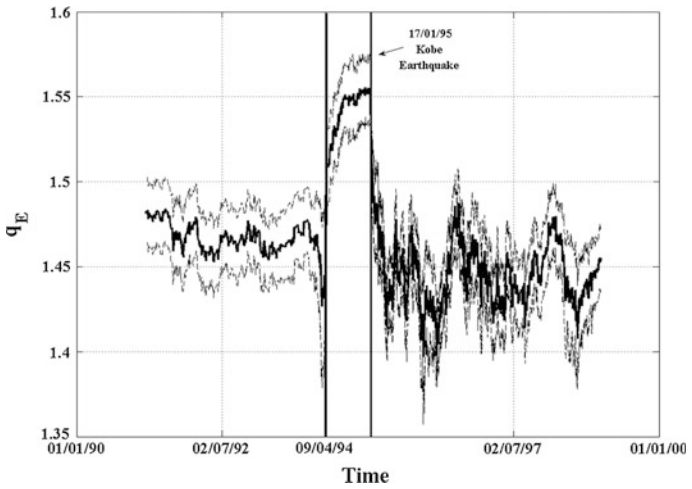

Fig. 25 Time variations of q_E values (*black continuous line*) over 200-event moving windows (*overlapping*), having a sliding factor equal to 1, and the associated standard deviation (*black dashed lines*). On April 9, 1994 the non-extensive parameter increases significantly, indicating the start of a transition phase towards the 1995 Kobe earthquake

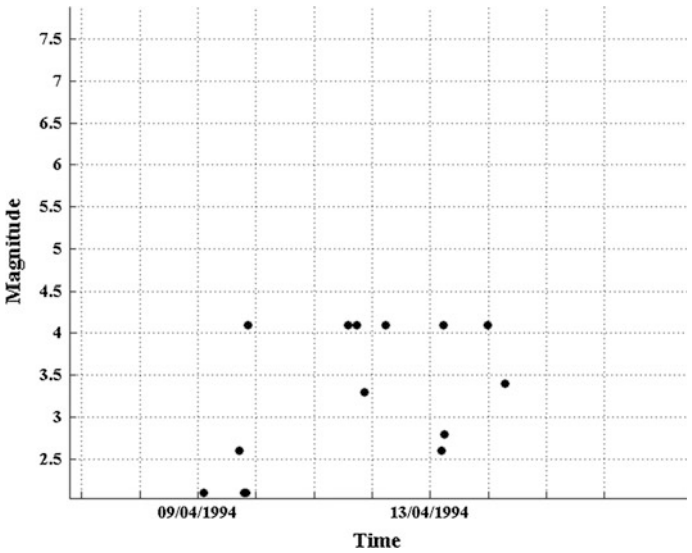

Fig. 26 Time distribution of seismicity, showing the occurrence of six seismic events equal to M = 4.1 between April 9, 1994 and April 13, 1994

Kobe earthquake. After the strong event the non-extensive parameter starts decreasing rapidly.

We detect a significant increase of the non-extensive parameter on April 9, 1994 which coincides with the occurrence of six seismic events equal to M = 4.1 (Fig. 26). The occurrence of these events breaks the magnitude pattern and along with the observed q_E variations indicates a transition phase towards the 1995 Kobe earthquake.

We conclude that the non-extensive statistical physics approach elucidates the physical evolution of a seismic area. Further development of the associated calculated thermostatistical parameter q_E as earthquake precursor improves our ability towards earthquake prediction and becomes beneficial for society and for communities experiencing earthquake hazard worldwide.

4 Quo Vademus?

Many aspects of seismology exhibit complexity. This is an area of research in both the geophysical and statistical physics communities. Although much progress has been made, many questions remain. Relevant areas include scaling laws, temporal and spatial correlations, critical phenomena, and nucleation. Within this complexity, scaling laws are now widely accepted. These include GR frequency–magnitude scaling, Omori's law for the decay of aftershock activity, and Bath's law relating

the magnitude of the largest aftershock to the magnitude of the main shock. It can be shown that GR scaling is equivalent to fractal scaling between the number of earthquakes and their rupture area. This scaling is scale invariant, it is robust, but do we understand it? One approach is to directly associate this scaling with the power-law slip-event scaling obtained in slider-block models. But in these models an individual slider block can participate in events of all sizes. This does not seem to be the case for earthquakes on faults; big faults appear to have large earthquakes and small faults small earthquakes. Thus, the GR scaling may be the consequence of a fractal distribution of fault sizes. This in turn can be attributed to scale-invariant fragmentation of the earth's brittle crust in active tectonic regions. The spatio-temporal distribution of seismicity also appears to be universally applicable, but why? A number of explanations have been given on an empirical basis. But the fundamental physics of this spatio-temporal pattern remains controversial.

Models relevant to earthquakes and complexity are at an early stage of development. Slider-block models have certainly played a role but are clearly only weakly related to distributed seismicity. Laboratory seismology also plays a role in understanding the complex behavior of brittle materials. Realistic simulations of distributed seismicity are just beginning to be developed. A major objective of these models is to provide estimates of the seismic hazard.

The study of the non-extensive statistical physics of earthquakes remains wide-open with many significant discoveries to be made. The philosophy is based on the holistic approach to understand the large scale patterns of seismicity. The link between this conceptual approach, based on the successes of statistical physics, and seismology thus remains a highly important domain of research. In particular, statistical seismology needs to evolve into a genuine physically-based statistical physics of earthquakes. In addition, more detailed and rigorous empirical studies of the frequency-size statistics of earthquake seismic moments and how they relate to seismo-tectonic conditions are needed in order to help settle the controversy over the power-law versus the characteristic event regime, and the role of regime-switching and universality. The important debate regarding statistical physics approaches to seismicity would benefit significantly from two points. Firstly, earthquake catalogs contain data uncertainties, biases and subtle incompleteness issues. Investigating their influence on the results of data analyses inspired by statistical physics, increases the relevance of the results. Secondly, the authors should make links with the literature on statistical seismology which deals with similar questions.

The results of the analysis in the cases described previously indicate that the ideas of non-extensive statistical physics can be used to express the non-linear dynamics that control the evolution of the earthquake activity at different scales. The physical models that have been derived using generalized statistical physics (NESP) can successfully describe the statistical properties of the earthquake activity, regarding the magnitude and spatio-temporal scales. These properties, as extracted from first principles, are important for the evolution of the earthquake activity and should be considered in any probabilistic seismic hazard assessment.

Since NESP approach can be evaluated in laboratory scale as well, a future challenging question is to understand how we can scale statistical physics laws in forecasting earthquakes or volcanic eruptions. The laboratory case is important, because it is likely to represent an ideal upper limit for the predictability of time-dependent failure in Earth materials and because many forecasting methodologies intuitively assume a simple scaling from laboratory to field conditions. The global effort to assess the predictability of earthquakes in a rigorous, prospective way has brought the lack of such rigorous evaluations into clearer focus. All forecasting models are subject to the effects of material heterogeneity, measuring error and incomplete data sampling. The key scientific challenge is to understand in a unified way, using NESP principles, the physical mechanisms that drive the evolution of fractures ensembles in laboratory and global scale and how we can use measures of evolution that will forecast the extreme fracture event rigorously and with consistency.

Acknowledgments The work was supported by the THALES Program of the Ministry of Education of Greece and the European Union in the framework of the project entitled "Integrated understanding of Seismicity, using innovative Methodologies of Fracture mechanics along with Earthquake and non-extensive statistical physics—Application to the geodynamic system of the Hellenic Arc. "SEISMO FEAR HELLARC", (MIS 380208).

References

Abe, S., & Suzuki, N. (2003). Law for the distance between successive earthquakes. *Journal of Geophysical Research, 108*(B2), 2113.

Abe, S., & Suzuki, N. (2005). Scale-free statistics of time interval between successive earthquakes. *Physica A, 350*, 588–596.

Bak, P., Christensen, K., Danon, L., & Scanlon, T. (2002). Unified scaling law for earthquakes. *Physical Review Letters, 88*, 178501.

Bak, P., & Tang, C. (1989). Earthquakes as a self-organized critical phenomenon. *Journal of Geophysical Research, 94*, 635–637.

Bak, P., Tang, C., & Wiesenfeld, K. (1987). Self-organized criticality: An explanation of 1/f noise. *Physical Review Letters, 59*, 381–384.

Bak, P., Tang, C., & Wiesenfeld, K. (1988). Self-organized criticality. *Physical Review A, 38*, 364–374.

Beck, C., & Schlogl, F. (1993). *Thermodynamics of chaotic systems: An introduction*. Cambridge: Cambridge University Press.

Bell, A. F., Naylor, M., & Main, I. G. (2013). Convergence of the frequency-size distribution of global earthquakes. *Geophysical Research Letters, 40*, 2585–2589.

Berrill, J. B., & Davis, R. O. (1980). Maximum entropy and the magnitude distribution. *Bulletin of the Seismological Society of America, 70*, 1823–1831.

Bird, P. (2003). An updated digital model of plate boundaries. *Geochemistry, Geophysics, Geosystems, 4*(3), 1027.

Burridge, L., & Knopoff, L. (1967). Model and theoretical seismicity. *Bulletin of the Seismological Society of America, 57*, 341–371.

Caruso, F., Pluchino, A., Latora, V., Vinciguerra, S., & Rapisarda, A. (2007). Analysis of self-organized criticality in the Olami-Feder-Christensen model and in real earthquakes. *Physical Review E, 75*, 055101.

Chakrabarti, B. K., & Benguigui, L. G. (1997). *Statistical physics of fracture and breakdown in disordered systems*. Oxford: Oxford Science Publications.

Corral, A. (2004). Long-term clustering, scaling, and universality in the temporal occurrence of earthquakes. *Physical Review Letters, 92*, 108501.

Darooneh, A. H., & Dadashinia, C. (2008). Analysis of the spatial and temporal distributions between successive earthquakes: Nonextensive statistical mechanics viewpoint. *Physica A, 387*, 3647–3654.

De Rubeis, V., Hallgas, R., Loreto, V., Paladin, G., Pietronero, L., & Tosi, P. (1996). Self-affine asperity model for earthquakes. *Physical Review Letters, 76*, 2599–2602.

Engdahl, E. R., & Villaseñor, A. (2002). Global seismicity: 1900–1999. International Handbook of Earthquake and Engineering Seismology, Part A, Chapter 41, (pp. 665–690). Academic Press, Waltham.

Ferri, G. L., Martínez, S., & Plastino, A. (2005). Equivalence of the four versions of Tsallis's statistics. *Journal of Statistical Mechanics: Theory and Experiment* P04009.

Gutenberg, B., & Richter, C. F. (1944). Frequency of earthquakes in California. *Bulletin of the Seismological Society of America, 34*, 185–188.

Hasumi, T. (2007). Interoccurrence time statistics in the two-dimensional Burridge-Knopoff earthquake model. *Physical Review E, 76*, 026117.

Hasumi, T. (2009). Hypocenter interval statistics between successive earthquakes in the two-dimensional Burridge-Knopoff model. *Physica A, 388*, 477–482.

Herrmann, H. J., & Roux, S. (1990). Modelization of fracture in disordered systems. *Statistical Models for the Fracture of Disordered Media* (pp. 159–188). Elsevier: North-Holland.

Hirata, T., & Imoto, M. (1991). Multifractal analysis of spatial distribution of micro earthquakes in the Kanto region. *Geophysical Journal International, 107*, 155–162.

Kagan, Y. Y. (1994). Observational evidence for earthquakes as a nonlinear dynamic process. *Physica D: Nonlinear Phenomena, 77*, 160–192.

Kagan, Y. Y. (1997). Seismic moment-frequency relation for shallow earthquakes: Regional comparison. *Journal of Geophysical Research, 102*, 2835–2852.

Kagan, Y. Y., & Jackson, D. D. (1991). Long-term earthquake clustering. *Geophysical Journal International, 104*, 117–133.

Kagan, Y. Y., & Jackson, D. D. (2000). Probabilistic forecasting of earthquakes. *Geophysical Journal International, 143*, 438–453.

Kagan, Y. Y., & Jackson, D. D. (2013). Tohoku earthquake: A surprise? *Bulletin of the Seismological Society of America, 103*, 1181–1194.

Kagan, Y. Y., & Knopoff, L. (1980). Spatial distribution of earthquakes: The two point correlation function. *Geophysical Journal Royal Astronomical Society, 62*, 303–320.

Kanamori, H. (1978). Quantification of earthquakes. *Nature, 271*, 411–414.

Kawamura, H., Hatano, T., Kato, N., Biswas, S., & Chakrabarti, B. K. (2012). Statistical physics of fracture, friction and earthquakes. *Review of Modern Physics, 84*, 839–884.

Knapmeyer, M., Oberst, J., Hauber, E., Wahlisch, M., Deuchler, C., & Wagner, R. (2006). Working model for spatial distribution and level of Mars' seismicity. *Journal of Geophysical Research, 111*, E11006.

Krajcinovic, D., & Van Mier, J. G. M. (2000). *Damage and fracture of disordered materials*. New York: Springer.

Lay, T., & Wallace, T. C. (1995). *Modern global seismology*. New York: Academic Press.

Lei, X. L., Kusunose, K., Nishizawa, O., Cho, A., & Satoh, T. (2000). On the spatiotemporal distribution of acoustic emissions in two granitic rocks under triaxial compression: the role of preexisting cracks. *Geophysical Research Letters, 27*, 1997–2000.

Lei, X., Nishizawa, O., Kusunose, K., & Satoh, T. (1992). Fractal structure of the hypocenter distribution and focal mechanism solutions of AE in two granites of different grain size. *Journal of Physics of the Earth, 40*, 617–634.

Lucchitta, B. K., McEwen, S., Clow, G. D., Geissler, P. E., Singer, R. B., Schultz, R. A., & Squyres, S. W. (1992). The canyon system of Mars. In H. H. Kieffer, B. M. Jakosky, C. W. Snyder, & M. S. Matthews (Eds.), *Mars* (pp. 453–492). USA: University of Arizona Press.

Main, I. (1996). Statistical physics, seismogenesis, and seismic hazard. *Reviews of Geophysics, 34*, 433–462.

Main, I. G., & Al-Kindy, F. H. (2002). Entropy, energy, and proximity to criticality in global earthquake populations. *Geophysical Research Letters, 29*(7), 25–1

Main, I. G., & Burton, P. W. (1984). Information theory and the earthquake frequency-magnitude distribution. *Bulletin of the Seismological Society of America, 74*, 1409–1426.

Main, I. G., Meredith, P. G., & Jones, C. (1989). A reinterpration of the precursory seismic b-value anomaly from fracture mechanics. *Geophysical Journal, 96*, 131–138.

Main, I. G., Meredith, P. G., & Sammonds, P. R. (1992). Temporal variations in seismic event rate and b-values from stress corrosion constitutive laws. *Tectonophysics, 211*, 233–246.

Mandelbrot, B. B. (1983). *The fractal geometry of nature*. San Francisco: Freeman.

Mège, D., & Masson, P. (1996). A plume tectonics model for the Tharsis province, Mars. *Planetary and Space Science, 44*, 1499–1546.

Michas, G., Vallianatos, F., & Sammonds, P. (2013). Non-extensivity and long-range correlations in the earthquake activity at the West Corinth rift (Greece). *Nonlinear Processes in Geophysics, 20*, 713–724.

Nature Debates. (1999). Nature debates: Is the reliable prediction of individual earthquakes a realistic scientific goal? Available from http://www.nature.com/nature/debates/.

Olami, Z., Feder, H. J. S., & Christensen, K. (1992). Self-organized criticality in a continuous nonconservative cellular automaton modeling earthquakes. *Physical Review Letters, 68*, 1244–1247.

Omori, F. (1894). On the aftershocks of earthquakes. *Journal of the College of Science*, *Imperial University of Tokyo 7*, 111–200.

Papadakis, G., Vallianatos, F., & Sammonds, P. (2013). Evidence of nonextensive statistical physics behavior of the Hellenic Subduction Zone seismicity. *Tectonophysics, 608*, 1037–1048.

Papadakis, G., Vallianatos, F., & Sammonds, P. (2014). A nonextensive statistical physics analysis of the 1995 Kobe earthquake, Japan. *Pure and Applied Geophysics* (accepted).

Picoli, S., Mendes, R. S., Malacarne, L. C., & Santos, R. P. B. (2009). q-distributions in complex systems: A brief review. *Brazilian Journal of Physics, 39*, 468–474.

Prigogine, I. (1980). *From being to becoming: Time and complexity in physical systems*. San Francisco: Freeman and Co.

Queirós, S. M. D. (2005). On the emergence of a generalised gamma distribution, application to traded volume in financial markets. *Europhysics Letters, 71*, 339–345.

Rundle, J. B., Gross, S., Klein, W., Ferguson, C., & Turcotte, D. L. (1997). The statistical mechanics of earthquakes. *Tectonophysics, 277*, 147–164.

Rundle, J. B., Turcotte, D. L., Shcherbakov, R., Klein, W., & Sammis, C. (2003). Statistical physics approach to understanding the multiscale dynamics of earthquake fault systems. *Reviews of Geophysics, 41*, 4.

Sammonds, P. (2005). Plasticity goes supercritical. *Nature Materials, 4*, 425–426.

Sammonds, P., & Ohnaka, M. (1998). Evolution of microseismicity during frictional sliding. *Geophysical Research Letters, 25*, 699–702.

Scholz, C. H. (1998). Earthquakes and friction laws. *Nature, 391*, 37–42.

Scholz, C. H., & Mandelbrot, B. B. (1989). *Fractals in geophysics*. Basel: Birkhuser.

Schultz, R. A. (1995). Gradients in extension and strain at Valles Marineris, Mars. *Planet Space Science, 43*, 1561–1566.

Schultz, R. A. (1997). Displacement–length scaling for terrestrial and Martian faults: Implications for Valles Marineris and shallow planetary grabens. *Journal of Geophysical Research, 102*, 12009–12015.

Schultz, R. A. (2003). Seismotectonics of the Amenthes Rupes thrust fault population, Mars. *Geophysical Research Letters, 30*, 1303–1307.

Schultz, R. A., Hauber, E., Kattenhorn, S., Okubo, C., & Watters, T. (2010). Interpretation and analysis of planetary structures. *Journal of Structural Geology, 32*, 855–875.

Shannon, C. E. (1948). A mathematical theory of communication. *Bell System Technical Journal 27*, 379–423, 623–656.

Silva, R., Franca, G. S., Vilar, C. S., & Alcaniz, J. S. (2006). Nonextensive models for earthquakes. *Physical Review E, 73*, 026102.

Sornette, D. (2004). *Critical phenomena in natural sciences, chaos, fractals, self-organization and disorder: Concepts and tools* (2nd ed.). Heidelberg: Springer.

Sornette, A., & Sornette, D. (1989). Self-organized criticality and earthquakes. *Europhysics Letters, 9*, 197–202.

Sotolongo-Costa, O., & Posadas, A. (2004). Fragment-asperity interaction model for earthquakes. *Physical Review Letters, 92*(4), 048501.

Telesca, L. (2010a). Analysis of Italian seismicity by using a nonextensive approach. *Tectonophysics, 494*, 155–162.

Telesca, L. (2010b). Nonextensive analysis of seismic sequences. *Physica A, 389*, 1911–1914.

Telesca, L. (2010c). A non-extensive approach in investigating the seismicity of L'Aquila area (central Italy), struck by the 6 April 2009 earthquake (ML = 5.8). *Terra Nova, 22*, 87–93.

Telesca, L. (2011). Tsallis-based nonextensive analysis of the southern California seismicity. *Entropy, 13*, 1267–1280.

Telesca, L. (2012). Maximum likelihood estimation of the nonextensive parameters of the earthquake cumulative magnitude distribution. *Bulletin of the Seismological Society of America, 102*(2), 886–891.

Telesca, L., Cuomo, V., Lapenna, V., Vallianatos, F., & Drakatos, G. (2001). Analysis of the temporal properties of Greek aftershock sequences. *Tectonophysics, 341*, 163–178.

Telesca, L., Lapenna, V., & Macchiato, M. (2003). Spatial variability of the time-correlated behaviour in Italian seismicity. *Earth and Planetary Science Letters, 212*, 279–290.

Telesca, L., Lapenna, V., & Vallianatos, F. (2002). Monofractal and multifractal approaches in investigating scaling properties in temporal patterns of the 1983–2000 seismicity in the western Corinth graben, Greece. *Physics of the Earth and Planetary Interiors, 131*, 63–79.

Tsallis, C. (1988). Possible generalization of Boltzmann-Gibbs statistics. *Journal of Statistical Physics, 52*, 479–487.

Tsallis, C. (2001). Non extensive statistical mechanics and its applications. In S. Abe, & Y. Okamoto (Eds.), Berlin: Springer.

Tsallis, C. (2009). *Introduction to nonextensive statistical mechanics: Approaching a complex world*. Berlin: Springer.

Tsallis, C., Bemski, G., & Mendes, R. S. (1999). Is re-association of folded proteins a case of non-extensivity? *Physics Letters A, 257*, 93–97.

Tsekouras, G. A., & Tsallis, C. (2005). Generalized entropy arising from a distribution of q indices. *Physical Review E, 71*, 046144.

Turcotte, D. L. (1997). *Fractals and chaos in geology and geophysics* (2nd ed.). Cambridge, UK: Cambridge University Press.

Utsu, T., Ogata, Y., & Matsura, R. S. (1995). The centenary of the Omori formula for a decay law of aftershock activity. *Journal of Physics of the Earth, 43*, 1–33.

Vallianatos, F. (2009). A non-extensive approach to risk assessment. *Natural Hazards and Earth System Sciences, 9*, 211–216.

Vallianatos, F. (2013). On the non-extensivity in Mars geological faults. *Europhysics Letters, 102*, 28006.

Vallianatos, F., Benson, P., Meredith, P., & Sammonds, P. (2012a). Experimental evidence of a non-extensive statistical physics behaviour of fracture in triaxially deformed Etna basalt using acoustic emissions. *Europhysics Letters, 97*, 58002.

Vallianatos, F., Kokinou, E., & Sammonds, P. (2011a). Non extensive statistical physics approach to fault population distribution. A case study from the Southern Hellenic Arc (Central Crete). *Acta Geophysica, 59*, 1–13.

Vallianatos, F., Michas, G., & Papadakis, G. (2014). Non-extensive and natural time analysis of seismicity before the M_w 6.4, 12 Oct 2013 earthquake in the south west segment of the Hellenic arc. (submitted).

Vallianatos, F., Michas, G., Papadakis, G., & Sammonds, P. (2012b). A non-extensive statistical physics view to the spatiotemporal properties of the June 1995, Aigion earthquake (M6.2) aftershock sequence (West Corinth rift, Greece). *Acta Geophysica, 60*, 758–768.

Vallianatos, F., Michas, G., Papadakis, G., & Tzanis, A. (2013). Evidence of non-extensivity in the seismicity observed during the 2011–2012 unrest at the Santorini volcanic complex, Greece. *Natural Hazards and Earth System Sciences, 13*, 177–185.

Vallianatos, F., & Sammonds, P. (2010). Is plate tectonics a case of non-extensive thermodynamics? *Physica A, 389*, 4989–4993.

Vallianatos, F., & Sammonds, P. (2011). A non-extensive statistics of the fault-population of the Valles Marineris extensional province, Mars. *Tectonophysics, 509*, 50–54.

Vallianatos, F., & Sammonds, P. (2013). Evidence of non-extensive statistical physics of the lithospheric instability approaching the 2004 Sumatran-Andaman and 2011 Honsu mega-earthquakes. *Tectonophysics, 590*, 52–58.

Vallianatos, F., & Triantis, D. (2012). Is pressure stimulated current relaxation in amphibolite a case of non-extensivity? *Europhysics Letters, 99*, 18006.

Vallianatos, F., Triantis, D., & Sammonds, P. (2011b). Non-extensivity of the isothermal depolarization relaxation currents in uniaxial compressed rocks. *Europhysics Letters, 94*, 68008.

Vallianatos, F., Triantis, D., Tzanis, A., Anastasiadis, C., & Stavrakas, I. (2004). Electric earthquake precursors: From laboratory results to field observations. *Physics and Chemistry of the Earth, 29*, 339–351.

Varotsos, P. A., Sarlis, N. V., & Skordas, E. S. (2001). Spatio-temporal complexity aspects on the interrelation between seismic electric signals and seismicity. *Practica of Athens Academy, 76*, 294–321.

Varotsos, P. A., Sarlis, N. V., & Skordas, E. S. (2011). *Natural time analysis: The new view of time, precursory seismic electric signals, earthquakes and other complex time series*. Berlin: Springer.

Vilar, C. S., Franca, G. S., Silva, R., & Alcaniz, J. S. (2007). Nonextensivity in geological faults. *Physica A, 377*, 285–290.

Wada, T., & Scarfone, A. M. (2005). Connection between Tsallis' formalisms employing the standard linear average energy and ones employing the normalized q-average energy. *Physics Letters A, 335*, 351–362.

Zaslavsky, G. M. (1999). Chaotic dynamics and the origin of statistical laws. *Physics Today, 52*, 39–45.